Effective hadron theories from a quark model in U(1) and SU(N) color

S. Gardner*
Center for Theoretical Physics, Laboratory of Nuclear Science and Department of Physics, Massachusetts Institute of Technology, Cambridge, Massachusetts 02139
and Institut für Theoretische Physik der Universität Heidelberg, Philosophenweg 19, D-6900 Heidelberg, Federal Republic of Germany
(Received 29 September 1989)

This is an extension of the earlier work of Gardner and Moniz [Phys. Rev. C **36**, 2504 (1987)] in the context of the quark-exchange model, in which effective hadron theories were constructed and their resulting physical observables were compared to the exact observables defined by the underlying quark model. The earlier U(1) study of the binding energy and form factor of a $q^2\bar{q}^2$ system is augmented, and it is extended in two different ways. First, the momentum distribution in U(1) color is now examined as well, since it is an observable which manifests behavior qualitatively distinct from that of an inert meson description; and, second, the hadronic theory construction is generalized to SU(N) color.

I. INTRODUCTION

In the context of electron-scattering experiments at small energy but large momentum transfers, that is, with $\omega \approx 0$ and q sufficient to probe the nucleus at distances less than a femtometer, it is natural to ask to what distance scale a hadronic picture of the nucleus may persist. Phenomenologically, the situation is unclear: heavier and heavier mesons must be included to describe processes at higher and higher momentum transfers, and the inclusion of each new meson requires the introduction of new parameters associated with the meson-baryon coupling constant and form factor. Moreover, slightly different parameter sets are required for the best phenomenological fit to different observables of the same nucleus, and the known extended size of the mesons and baryons makes such a picture also intuitively unclear. However, the large-N limit of quantum chromodynamics (QCD) is a theory of mesons; this strengthens the notion that this basis is apt,[3,4] though it is unclear if $N=3$ is sufficiently large for the properties of the infinite-color limit to be germane.

Issues of effective hadron theory convergence can be addressed in the context of a quark model. The basic logic of this paper and its predecessor (see Ref. 1) is (i) to choose a physically appealing quark model which is numerically exactly solvable for a simple multiquark system, (ii) to construct an equivalent hadron theory from the underlying quark model, and, finally, (iii) to compute and compare the observables of the quark model with those of the chosen effective theory upon the inclusion of successive hadron excited states. An effective hadron theory is constructed in a projection-operator approach; it is an "equivalent" theory if solution of the infinite-coupled-channel problem in the hadronic basis yields observables identical to those of the quark model. It is to be emphasized that the choice of a hadronic scheme itself is somewhat arbitrary, just as it is impossible to define a single hadron unambiguously when two hadrons overlap; however, once the confined coordinates and corresponding confined, or hadron, wave functions are chosen, the derivation of the effective theory proceeds unambiguously. Thus, the comparison between the quark and a particular hadronic language is crisp and is not subject to uncontrolled ambiguities. The comparison of the quark-model observables with those of various hadronic schemes is meant to determine not only if a rapidly convergent hadronic scheme exists, but also if such a description is unique.

The quark model used is the quark-exchange model of Lenz *et al.* for a $q^2\bar{q}^2$ system, and, in the face of the technical difficulties of QCD, it is appealing for such a study as it is numerically exactly solvable but yet also has saturating and confining interactions.[2] The quark-exchange model is a "minimal" dynamical extension of traditional nonrelativistic potential quark models, which have been rather successful in reproducing static hadronic properties such as masses and decay widths.[5] The model is constructed for the general case of SU(N) color. Only overall color singlet hadron states are ever considered; color space is thus partitioned into color singlet states with color singlet hadrons and color singlet states with color nonsinglet hadrons. This latter set of states shall henceforth be referred to as the hidden color sector. In this many-body model, the SU(N) interactions are not specified by confinement, and two parameters are needed. The first, ν_c, specifies the propagation length of the hidden color states relative to the singlet states, and the second, λ, which depends on the number of colors N and the overall symmetry of the wave function, determines the relative contribution of the hidden color sector. This model is "minimal" as in the color singlet sector it presumes the Hamiltonian of the isolated hadrons to persist throughout the "interaction region," the extent of which is determined by the confinement scale. The hidden color sector does not have such a constraint on its interactions, but it may contribute explicitly to the Hamil-

tonian only in the region determined by ν_c, the single dynamical parameter in the model. The U(1) limit, however, contains just the confining dynamics determined from isolated hadron spectroscopy. The many-body nature of the potential allows confinement to be enforced without introducing the long-range van der Waals forces typical of two-body potential models;[6] thus, the interactions are saturating and conform in this qualitative way to empirical data.[7]

As noted already, the model yields a surprisingly rich set of phenomena.[2] In the specific example of a $q^2\bar{q}^2$ system, which is technically simplest and yet contains the qualitative features of more complicated systems, one finds that the scattering in the system exhibits resonances at the inelastic hadronic thresholds and that a weak deuteronlike bound state exists with a binding energy of only a few percent of the hadron excitation energy scale. This is true not only in SU(N) color when ν_c and λ are chosen "reasonably," but also in the U(1) limit. The U(1) limit is technically much simpler to treat; it is a convenient toy model in which to explore the consequences of saturating, confining dynamics.

The original paper of Gardner and Moniz examined effective hadron theory convergence in the U(1) limit to the binding energy, elastic form factor, and low-energy scattering parameters of a $q^2\bar{q}^2$ system.[1] They concluded that it is possible to find hadronic schemes which reproduce all of the above quark-model observables. At least two different successful hadronic schemes exist, and, moreover, the two that were found are qualitatively quite different. In the augmented study of the U(1) case here, these differences are illustrated analytically, via asymptotic analysis of the effective potentials and effective charge operators. The earlier U(1) color work is also extended to SU(N) interactions. In this model, the inclusion of color nonsinglet forces makes any $N>1$ case qualitatively different from the U(1) limit. To this purpose, the $N=2$ and 3 cases are not dissimilar, and the choice of the color hidden forces is tailored to the expectation that $N=2,3$ is small in comparison to an infinite number of colors. One can examine the binding energy, low-energy scattering parameters, and elastic form factor as in Ref. 1, but technical limitations in the SU(N) color case prevent an exhaustive study in $N=3$. Thus, the $N=2$ case is considered as well. In light of the success of the earlier U(1) study in producing hadronic schemes which fit the studied quark-model observables and in anticipation of some success in a similar study in $N=2,3$, it is reasonable to seek out other observables which could be more sensitive to the underlying dynamics. The quark momentum distribution is certainly a candidate; this observable is distinct from the observables studied earlier in that it has qualitatively different behavior from an inert meson description, or package model. This observable is readily studied in the U(1) limit; it is of interest, then, to see whether this additional observable poses a more stringent test for the successful hadronic schemes previously considered. Consequently, it is sensible to examine the U(1) limit in some detail before continuing to the full SU(N) problem. For clarity, some of the earlier results of Gardner and Moniz are included.[1]

II. THE QUARK-EXCHANGE MODEL

The quark-exchange model is a nontrivial, yet tractable, realization of a saturating and confining quark theory. The model has been reviewed extensively in Ref. 2; interested readers may find further details there.

Here I shall consider a $q^2\bar{q}^2$ system with harmonic confinement in three space dimensions. The $\bar{q}$'s are not required to be antiquarks but merely objects distinguishable from quarks. The formulation of the model relies on the introduction of projection operators which simultaneously act in color and configuration space. For the $q^2\bar{q}^2$ system, for quarks 1,2 and antiquarks $\bar{1},\bar{2}$ with positions $\mathbf{r}_i$, one convenient choice of projectors is[2]

$$P_I = P_I^C \Theta(r_{1\bar{2}}^2 + r_{2\bar{1}}^2 - r_{1\bar{1}}^2 - r_{2\bar{2}}^2) , \tag{1a}$$

$$\tilde{P}_I = \tilde{P}_I^C \Theta(r_{1\bar{1}}^2 + r_{2\bar{2}}^2 - r_{1\bar{2}}^2 - r_{2\bar{1}}^2) , \tag{1b}$$

where $\mathbf{r}_{ij} \equiv \mathbf{r}_i - \mathbf{r}_j$, and the superscript C operators which act purely in color SU(N) space are

$$P_I^C = |(1,\bar{1})_I (2,\bar{2})_I\rangle_0 \langle (1,\bar{1})_I (2,\bar{2})_I|_0 \equiv |I\rangle\langle I| \tag{2a}$$

and

$$\tilde{P}_I^C = |(2,\bar{1})_I (1,\bar{2})_I\rangle_0 \langle (2,\bar{1})_I (1,\bar{2})_I|_0 \equiv |\tilde{I}\rangle\langle \tilde{I}| . \tag{2b}$$

The projectors in Eq. (1) are orthogonal and complete in the space of overall color singlets. I may be 0 or 1. The 0 subscript denotes the color singlet state constructed from color singlet clusters, and the 1 subscript denotes a sum over the color singlet states constructed from the possible combinations of color nonsinglet clusters. A potential which satisfies the necessary requirements is

$$V = V_2 \tilde{P}_0 + V_1 P_0 + [\tfrac{1}{2}(V_1+V_2)+W_1]P_1 + [\tfrac{1}{2}(V_1+V_2)+W_2]\tilde{P}_1 , \tag{3}$$

where $V_1 = v(1,\bar{1}) + v(2,\bar{2})$, $V_2 = v(2,\bar{1}) + v(1,\bar{2})$, and the $v(i,j)$ are overall confining potentials between quark i and antiquark j. The hidden color potentials W_1 and W_2 are essentially arbitrary: one merely requires that the combinations $\frac{1}{2}(V_1+V_2)+W_1$ and $\frac{1}{2}(V_1+V_2)+W_2$ are confining. The W_i's are not constrained by isolated hadron spectroscopy. Equation (3) is saturating by ansatz; the projection operators act to insure that, in the color singlet sector, only noninteracting $q\bar{q}$ pairs exist away from the rearrangment surface, the surface in configuration space where the quark content changes, or, equivalently, where the q-$\bar{q}$ "strings" flip [i.e., the surface defined by vanishing arguments in the Θ functions of Eq. (1)]. In this model, at any point in color and configuration space, the quarks are clustered into $q\bar{q}$ pairs; however, only in the color singlet sector are the $q\bar{q}$ pairs constrained to be noninteracting. Thus, the only dynamics in the color singlet sector comes from the exchange of quarks along the rearrangment surface; this physics is maximized in s-wave processes, which are what I shall consider.

Now for harmonic confinement, the isolated meson Hamiltonian is

$$H=-\frac{1}{2\mu}\Delta+\tfrac{1}{2}\mu\omega^2 r^2 , \tag{4}$$

where $\mu=\frac{1}{2}m_q$ and r is the relative coordinate. Introducing center of mass and relative coordinates,

$$\mathbf{r}_{\text{c.m.}}=\tfrac{1}{4}(\mathbf{r}_1+\mathbf{r}_2+\mathbf{r}_3+\mathbf{r}_4) , \tag{5a}$$

$$\mathbf{x}=\tfrac{1}{2}(\mathbf{r}_1+\mathbf{r}_2)-\tfrac{1}{2}(\mathbf{r}_3+\mathbf{r}_4) , \tag{5b}$$

$$\mathbf{y}=\tfrac{1}{2}(\mathbf{r}_1+\mathbf{r}_3)-\tfrac{1}{2}(\mathbf{r}_2+\mathbf{r}_4) , \tag{5c}$$

$$\mathbf{z}=\tfrac{1}{2}(\mathbf{r}_1+\mathbf{r}_4)-\tfrac{1}{2}(\mathbf{r}_2+\mathbf{r}_3) , \tag{5d}$$

and using units $\hbar=2m=b_0=1$ (so that $\omega=4$), one obtains the Hamiltonian

$$H(\mathbf{x},\mathbf{y},\mathbf{z})=-\Delta_x-\Delta_y-\Delta_z+V(\mathbf{x},\mathbf{y},\mathbf{z}) , \tag{6}$$

where

$$V(\mathbf{x},\mathbf{y},\mathbf{z})=2[2x^2+y^2+z^2-(y^2-z^2)P_0-(z^2-y^2)\tilde{P}_0 + W_1(\mathbf{x},\mathbf{y},\mathbf{z})P_1+W_2(\mathbf{x},\mathbf{y},\mathbf{z})\tilde{P}_1] . \tag{7}$$

In the color singlet sector, the dependence on the confined variable $\mathbf{x}$ factorizes, and the y,z orbital angular momenta decouple, as a consequence of the harmonic confinement.

As the requirements that $\frac{1}{2}(V_1+V_2)+W_1$ and $\frac{1}{2}(V_1+V_2)+W_2$ are confining pose an insufficient constraint, the actual choice of the W_i's is motivated by convenience. Following Ref. 2, one presumes that the color singlet and nonsinglet interactions have the same harmonic form and chooses pure $q-q$ and $\bar{q}-\bar{q}$ interactions to find

$$W_1=W_2=u_c(r_{12}^2+r_{\bar{1}\bar{2}}^2)=2u_c(y^2+z^2) \tag{8}$$

with u_c an arbitrary constant, so that

$$V(x,y,z)=4[x^2+z^2P_0+y^2\tilde{P}_0+\nu_c^2(y^2+z^2)(P_1+\tilde{P}_1)] . \tag{9}$$

This choice of W_i preserves the angular-momentum decoupling. The constant $\nu_c^2=(1+u_c)/2$ specifies the physical extent of the color nonsinglet sector relative to the color singlet one, and calculations will be made for varying ν_c in order to gauge the sensitivity of the results to the strength of the hidden color interactions. For low-energy observables, I shall consider the s-wave Hamiltonian

$$h(y,z)=-\partial_y^2-\partial_z^2+4[z^2P_0+y^2\tilde{P}_0 +\nu_c^2(y^2+z^2)(P_1+\tilde{P}_1)] , \tag{10}$$

where the x dependence has been dropped, because that coordinate decouples. In the U(1) limit, this merely becomes

$$h(y,z)=-\partial_y^2-\partial_z^2+4[z^2\Theta(y-z)+y^2\Theta(z-y)] . \tag{11}$$

Masutani has pointed out that this particular choice of the hidden color interactions leads to nonvanishing interactions for large N and has studied a quark-exchange model whose hidden color interactions have the appropriate large-N behavior.[3,4,8] His model, though, has no bound state for $N>1$, so that I have chosen to study the color dynamics used in Ref. 2, since they admit a richer set of observables.

Solutions to Eqs. (10) and (11) can be classified with respect to their symmetry under y,z exchange. Consideration can thus be restricted to the $y\geq z$ triangle in the (y,z) scattering plane. Thus, $h_{\text{SU}(N)}(y,z)$ can be broken into singlet, 0, and hidden color singlet, 1, components

$$h_0(y,z)=-\partial_y^2-\partial_z^2+4z^2 , \tag{12a}$$

$$h_1(y,z)=-\partial_y^2-\partial_z^2+4\nu_c^2(z^2+y^2) , \tag{12b}$$

where

$$\Psi(y,z)=\Psi_0(y,z)|0\rangle+\Psi_1(y,z)|1\rangle .$$

Using the transformation properties of the $|\tilde{I}\rangle$ to $|I\rangle$ basis under SU(N), one finds the boundary conditions at $y=z=t$

$$\frac{\Psi_1(t,t)}{\Psi_0(t,t)}=-\frac{\alpha-s}{\beta} , \tag{13a}$$

$$\frac{\partial_n\Psi_1(t,t)}{\partial_n\Psi_0(t,t)}=-\frac{\alpha+s}{\beta} , \tag{13b}$$

where $\alpha=1/N$, $\beta=(1-\alpha^2)^{1/2}$, s is the symmetry of the wave function under y,z exchange, and the normal derivative $\partial_n\equiv\partial_y-\partial_z$ is evaluated at $y=z=t$. The components of Eq. (12) are coupled by virtue of the boundary condition on $z=y$. In the U(1) limit, only the symmetric state, that is, with $\partial_n\Psi(t,t)=0$, has a bound state, and that is the state whose observables shall be considered. The SU(N) problem is distinct, then, from the U(1) not only in the explicit addition of the hidden color sector but also in the novel boundary condition along the diagonal which couples the singlet and hidden color singlet components of the wave function. With the additional requirements of regularity in Ψ_0 and Ψ_1 as $y,z\to 0$ and of confinement in Ψ_1 and scattered-wave boundary conditions in Ψ_0 as $y,z\to\infty$, the problem in both U(1) and SU(N) is fully specified, and one can use Green's theorem to find an integral equation for $\Psi(y,z)$. The scattering phase shifts and bound-state energies, as well as the form factors and bound-state momentum distributions, can then be calculated; see Ref. 2 for details.

Some physical insight into the behavior of the SU(N) scattering phase shifts and bound-state energies with ν_c can be gleaned if one considers the eigenstates of the hidden color Hamiltonian, Eq. (12b), alone. The bound-state energies in the absence of any coupling to the color singlet sector are

$$\varepsilon_{mm'}=4\nu_c[3+2(m+m')] .$$

The isolated hadron Hamiltonian has bound-state energies $\varepsilon_n=4(\frac{3}{2}+2n)$, so that the numerical results can be organized roughly according to whether or not ν_c exceeds the value of 0.5, the value for which the hidden

color ground state is at elastic threshold. For $\nu_c \leq 0.5$, the hidden color ground state generates an attraction, regardless of N or s. For $\nu_c \gg 0.5$, the interaction with the hidden color ground state is purely repulsive, and for sufficiently large ν_c the bound state is destroyed. For $\nu_c \gtrsim 0.5$, the interaction between the U(1) bound state and the hidden color wave function is extremely sensitive to N and s, and it is here that the phase shifts and scattering lengths have their most dramatic behavior. Consequently, it is upon this region in ν_c parameter space that I shall concentrate.

The bound-state form factor in SU(N) is

$$F(q)=F_0(q)+F_1(q) , \tag{14a}$$

$$F_I(q)=2e^{-q^2/32}\int_0^\infty dy \int_0^y dz\, j_0(qy/2)j_0(qz/2) \times[\psi_I(y,z)]^2 , \tag{14b}$$

where the decoupled x oscillator is assumed to be in its ground state and the sum of the charges of the quarks and antiquarks is taken to be 1. The hidden color sector contributes explicitly to the total form factor in the form of $F_1(q)$. For technical convenience, only the color singlet form factor based on color singlet mesons, $F_0(q)$, will be considered in SU(N). In this case, the influence of the hidden color sector is only felt in the boundary condition imposed on the color singlet sector wave function Ψ_0. It may be artificial to examine the hadronic convergence of only a single component, but it does form a necessary constraint. It is clear that convergence in the total form factor cannot exist unless there is a convergence in each of the pieces.

In the U(1) limit, the total form factor is merely Eq. (14b) with Ψ_I the color singlet bound-state wave function $\Psi_B(y,z)$. The momentum distribution of the quark model in this limit is

$$n(p)=8\int d^3p_{(x)}\, d^3p_{(y)}\, d^3p_{(z)}\delta^{(3)}(\mathbf{p}_{(x)}+\mathbf{p}_{(y)}+\mathbf{p}_{(z)}-2\mathbf{p}) \times|\tilde{\phi}_0(\mathbf{p}_{(x)})|^2|\tilde{\Psi}(\mathbf{p}_{(y)},\mathbf{p}_{(z)})|^2 . \tag{15}$$

Including the $\mathbf{p}_{(x)}$ contribution

$$|\tilde{\phi}_0(\mathbf{p}_{(x)})|^2=(2\pi)^{-3/2}\exp(-p_{(x)}^2/2) ,$$

one has

$$n(p)=\left[\frac{2}{\pi}\right]^{3/2}\int d^3p_{(y)}\, d^3p_{(z)} \times e^{-(2\mathbf{p}-\mathbf{p}_{(y)}-\mathbf{p}_{(z)})^2/2}\tilde{\Psi}^2(\mathbf{p}_{(y)},\mathbf{p}_{(z)}) , \tag{16}$$

where

$$\tilde{\Psi}(\mathbf{p}_{(y)},\mathbf{p}_{(z)})=\left[\frac{1}{2\pi}\right]^3\int d^3y\, d^3z\, e^{i(\mathbf{p}_{(y)}\cdot\mathbf{y}+\mathbf{p}_{(z)}\cdot\mathbf{z})}\tilde{\Psi}(\mathbf{y},\mathbf{z}) \tag{17}$$

and

$$\tilde{\Psi}(\mathbf{y},\mathbf{z})=\frac{1}{4\pi yz}\Psi_B(y,z) .$$

Following Ref. 2, the second moment of this distribution can be calculated straightforwardly using virial theorem arguments. Consider the commutator of the dilatation operator with the Hamiltonian. That is, for any $|\Psi\rangle$,

$$\begin{aligned}\langle\Psi|[\mathbf{x}\cdot\mathbf{p}_{(x)}+\mathbf{y}\cdot\mathbf{p}_{(y)}+\mathbf{z}\cdot\mathbf{p}_{(z)},H]|\Psi\rangle &=2i[\langle\Psi|p_{(x)}^2+p_{(y)}^2+p_{(z)}^2-V|\Psi\rangle] \\ &=2i[2\langle\Psi_B|p_{(x)}^2+p_{(y)}^2+p_{(z)}^2|\Psi_B\rangle-(12+\varepsilon_B)] .\end{aligned} \tag{18}$$

H and V are given in Eq. (6) in the limit of U(1) color with s waves only. The second line of Eq. (18) follows for the bound-state wave function Ψ_B; ε_B is the binding energy and 12 is the zero point energy. From Eq. (15), one can show that, for s waves,

$$\langle p^2\rangle=\tfrac{1}{4}(\langle p_{(x)}^2\rangle+\langle p_{(y)}^2\rangle+\langle p_{(z)}^2\rangle) . \tag{19}$$

Noting that the left-hand side of Eq. (18) is identically zero for the $q^2\bar{q}^2$ bound state and using Eq. (19) yields

$$\begin{aligned}\langle p^2\rangle_{\text{quark}} &=\tfrac{3}{2}+\tfrac{1}{8}\varepsilon_B \\ &=1.4800\end{aligned} \tag{20}$$

as $\varepsilon_B=-0.160$.[2] It is useful to compare this result with the second moment of the momentum distribution of the $q^2\bar{q}^2$ system at asymptotic separations. If y is infinite,

$$h_{\text{isol}}=-\partial_x^2-\partial_z^2+4x^2+4z^2$$

$\forall z$. Then

$$\begin{aligned}n_{\text{isol}}(p) &=8\int d^3p_1\, d^3p_2\delta^{(3)}(\mathbf{p}_1+\mathbf{p}_2-2\mathbf{p})|\tilde{\phi}_0(\mathbf{p}_1)|^2|\tilde{\phi}_0(\mathbf{p}_2)|^2 \\ &=\pi^{-3/2}e^{-p^2} ,\end{aligned} \tag{21}$$

where $|\tilde{\phi}_0(\mathbf{p})|^2$ is as before. This is identical to the momentum distribution of a single isolated hadron. The above expression finally yields $\langle p^2\rangle_{\text{isol}}=\frac{3}{2}$. Thus, $\langle p^2\rangle_{\text{quark}}$ is less than the isolated meson value; this is a consequence of the existence of the $q^2\bar{q}^2$ bound state and the virial theorem. The harmonic confinement in this model implies that $\langle T\rangle=\langle V\rangle$, and since the $q^2\bar{q}^2$ state considered is bound relative to the asymptotic $q\bar{q}$ states, $\langle p^2\rangle$ must decrease as well. In an inert meson description, one can show that the second moment is necessarily a sum of the $\langle p^2\rangle$ of the inert meson and that of the wave function of the relative motion; thus, the total $\langle p^2\rangle$ is necessarily increased over that of the isolated hadron itself. The decrease of $\langle p^2\rangle$ observed, then, cannot be produced in any package model; rather, it arises from the exchange dynamics and the virial theorem at the quark level.

The quark-model results introduced in this section will serve as the "experiment" for the observables calculated from the effective hadron theories to follow.

III. U(1) HADRONIZATION

A. Schemes

Here I shall discuss the hadronization of the U(1) theory. Many of the fundamental considerations discussed here follow for the SU(N) case as well.

To construct an equivalent hadronic theory, it is necessary to identify a confined variable which will be associated with the hadron internal degrees of freedom. Projecting out these internal degrees of freedom leads to a description of the original quark model in terms of residual interactions between hadrons. These are a function of the channel variable, which specifies the relative hadron separation. This entire procedure is necessarily nonunique: no unique definition of a hadron exists when two hadrons overlap as one cannot identify which hadron should contain which quark, nor does a unique prescription exist for the channel variable.

Given a choice of confined and channel variables, one must then establish a machinery for separation of the degrees of freedom associated with each of the coordinates. This is most readily accomplished in a projection-operator formalism. After a choice of the confined coordinate, a complete set of hadron internal wave functions can be defined. The confined coordinate definition may depend implicitly on the channel coordinate, and the internal wave functions may have this dependence as well. It is essential to choose confined wave functions that map to the isolated hadron spectrum at infinite separation; there exists no further constraint on their definition. The projection operator constructed from these wave functions finally defines the hadronic scheme. If the confined basis is complete and orthonormal, one can construct a projector P_n which satisfies $\sum_n P_n^2=1$, $P_n P_m=\delta_{nm}P_n$. The observables of the U(1) quark model, such as the bound-state energy and form factor

$$\varepsilon=\langle \Psi_B|\hat{\mathbf{h}}_{\mathrm{U}(1)}|\Psi_B\rangle \ , \tag{22}$$

$$F(q)=\langle \Psi_B|\hat{\rho}_q|\Psi_B\rangle \ , \tag{23}$$

can thus be rewritten

$$\varepsilon=\sum_{n,m}\langle \Psi_B|P_n(P_n\hat{\mathbf{h}}_{\mathrm{U}(1)}P_m)P_m|\Psi_B\rangle \ , \tag{24}$$

$$F(q)=\sum_{n,m}\langle \Psi_B|P_n(P_n\hat{\rho}_q P_m)P_m|\Psi_B\rangle \ . \tag{25}$$

Here $\hat{\rho}_q$ is the quark-model charge operator. Now $P_m|\Psi_B\rangle$ defines an effective hadronic wave function $|\chi_m\rangle$, $P_n\hat{\rho}_q P_m$ an effective hadronic charge operator $[\hat{\rho}_q]_{\mathrm{nm}}$, and $P_n\hat{\mathbf{h}}_{\mathrm{U}(1)}P_m$ an effective coupled-channel Hamiltonian $[\hat{\mathbf{h}}_{\mathrm{U}(1)}]_{nm}$. The m subscript corresponds to a hadron in its mth internal state. Self-consistency of the hadronic operator and wave-function expansion is implicit. (One could consider different expansions for the operators and wave functions using projectors P and $\tilde{P}$, say, but this is unnatural as $\langle P_n|\tilde{P}_m\rangle\neq\delta_{nm}$, in general.) The channel wave function $|\chi_m\rangle$ is formally defined as an integral over the projector times the quark-model wave function. In practice, however, Eq. (24) is rewritten as

$$\varepsilon=\sum_{n,m}\langle \chi_n|[\hat{\mathbf{h}}_{\mathrm{U}(1)}]_{nm}|\chi_m\rangle \tag{26}$$

and solved as a coupled-channel problem for the energy and channel wave functions to a given level of truncation. If the confined and channel wave functions contain all the boundary conditions of the original quark model, a sum over all the terms in the hadronic expansion—and solution of the infinite coupled-channel problem—will yield the quark-model binding energy and form factor. Ultimately, though, one is not interested in whether or not the hadronic expansion is precisely equivalent to the quark-level description, but, rather, whether or not the expansion can approximately reproduce the quark-model results after the inclusion of just a few terms.

As shown in Ref. 1, incorporation of the quark-exchange dynamics in the hadronization scheme is crucial. Thus, rather than merely picking either y or z as the confined coordinate, only confined coordinates which depend on the dynamics will be considered. For y and z coordinates, the quark-model potential acts in z for $y>z$ and in y for $z>y$ [see Eq. (11)]. One choice, then, which recognizes the quark-model rearrangement, is to use z as the confined coordinate for $y>z$ and y for $z>y$. With this confined coordinate definition, confined wave functions can be defined which incorporate the dynamics by measure of the imposed rearrangement surface boundary conditions. The definition of a hadron is modified at finite separation from its free value; this modification is arbitrary as such a definition is unclear when hadrons overlap. As one specific choice, consider the confined wave functions $\varphi_n(z;y)$ for $y\geq z$ such that

$$(-\partial_z^2+4z^2)\varphi_n(z;y)=\varepsilon_n(y)\varphi_n(z;y) \ , \tag{27}$$

where $\partial_z\varphi_n(z;y)|_{z=y}=0$, and the $\varphi_n(z;y)$, which are real, satisfy

$$\int_0^y dz\,\varphi_n(z;y)\varphi_m(z;y)=\delta_{nm} \ .$$

For $y\to\infty$, $\varphi_n(z;y)\to\phi_n(z)$, where the $\phi_n(z)$ are the eigenstates of the isolated hadron Hamiltonian $-d^2/dz^2+4z^2$. One would like to embed the exact condition at $z=y$ and I shall consider such a choice below; however, for these coordinates, the normal derivative at $z=y$ couples the confined and channel wave functions. Thus, for technical convenience, only a constraint on the z derivative is made at $z=y$. The wave function should vary slowly in the y direction for a weakly bound state: this is the physical basis for the approximation made. Thus, this particular hadronic expansion $\forall n,m$ does not converge to the quark-model wave function; however, contingent on the viability of the above physical approximation, a few-channel truncation may be a reasonable representation of its observables.

An alternative scheme may be defined that incorporates not only the quark rearrangement but also the exact boundary condition at $z=y$. Thus, this latter scheme shall truly be an equivalent hadronic theory. I do this not merely to see whether a better quantitative description of the observables can be obtained, but, rather, to examine whether other "reasonable" hadronization schemes can yield good convergence to the underlying quark-model observables. Consider a transformation such that the confined coordinate becomes the normal coordinate at the rearrangement surface $z=y$. One simple choice is that of polar coordinates: for $y\geq z$, consider (r,θ) such that $y=r\cos\theta$, $z=r\sin\theta$. This maps the quark-level Hamiltonian $h(y,z)$ to

$$h(r,\theta)=-\partial_r^2-\frac{1}{r}\partial_r-\partial_\theta^2+4r^2\sin^2\theta \ . \tag{28}$$

In analogy to Eq. (27) with $z=r\theta$, confined wave functions $\varphi_n(\theta;r)$ are introduced for $\theta\le\pi/4$ such that

$$\left[-\frac{1}{r^2}\partial_\theta^2+4r^2\theta^2\right]\varphi_n(\theta;r)=\varepsilon_n(r)\varphi_n(\theta;r) \ , \tag{29}$$

where $\partial_\theta\varphi_n(\theta;r)|_{\pi/4}=0$ and

$$\int_0^{\pi/4} r d\theta\,\varphi_m(\theta;r)\varphi_n(\theta;r)=\delta_{nm} \ .$$

For convenience, the confined wave functions have been defined with a $(r\theta)^2$ potential, which is what $r^2\sin^2\theta$ becomes for $z\ll y$. For large r, $\varphi_n(\theta;r)\sim\phi_n(r\theta)$, so that the isolated hadron spectrum is recovered in this limit. Here the Jacobian factor of r can be trivially incorporated in the confined wave function normalization since it has no θ dependence. The $(1/r)\partial_r$ term in $h(r,\theta)$ suggests the presence of unphysical long-range effective forces; nevertheless, I shall proceed to study the observables of this scheme.

The two schemes just described were previously introduced in Ref. 1. I shall refer to the (y,z) and (r,θ) schemes as I and II, respectively. Using the confined wave functions as above, one can define the following hadronic projectors. For scheme I,

$$\begin{aligned}P_n^{(\mathrm{I})}(y,z,y',z')=&[\varphi_n(z;y)\varphi_n(z';y')\delta(y-y')\\&\times\theta(y-z)\theta(y'-z')\\&+\varphi_n(y;z)\varphi_n(y';z')\delta(z-z')\\&\times\theta(z-y)\theta(z'-y')] \ .\end{aligned} \tag{30}$$

The functions $\varphi_n(y;z)$ for $y\in[0,z]$ follow from the $\varphi_n(z;y)$ with $z\leftrightarrow y$. For scheme II,

$$P_n^{(\mathrm{II})}(\theta,r,\theta',r')=\sqrt{rr'}\varphi_n(\theta;r)\varphi_n(\theta';r')\delta(r-r') \ . \tag{31}$$

This projector holds for all θ. The rearrangement is embedded in the coordinate definition: for $\theta\ge\pi/4$, one chooses $z=r\cos\theta$ and $y=r\sin\theta$. These projectors can now be inserted in the exact matrix element for the energy to derive a complete set of coupled-channel equations for each scheme. Defining the channel wave functions,

$$\chi_n(y)\equiv\sqrt{2}\int_0^y dz\,\varphi_n(z;y)\Psi_B(z,y) \ ,$$

so that

$$\begin{aligned}\Psi_B(z,y)=\frac{1}{\sqrt{2}}\sum_n[&\chi_n(y)\varphi_n(z;y)\theta(y-z)\\&+\chi_n(z)\varphi_n(y;z)\theta(z-y)]\end{aligned} \tag{32}$$

or, equivalently, in scheme II, defining

$$\chi_n(r)\equiv\sqrt{2}\int_0^{\pi/4} r d\theta\,\varphi_n(\theta;r)\Psi_B(\theta,r) \ ,$$

so that, for $\theta\le\pi/4$,

$$\Psi_B(\theta,r)=\frac{1}{\sqrt{2}}\sum_n\left[\chi_n(r)\varphi_n(\theta;r)\Theta\left[\frac{\pi}{4}-\theta\right]\right] \ , \tag{33}$$

one finally obtains from Eq. (24)

$$\begin{aligned}\varepsilon=&\tfrac{1}{4}\sum_{n,m}(\langle\chi_m\varphi_m|h\varphi_n\chi_n\rangle+\langle\chi_n\varphi_n|h\varphi_m\chi_m\rangle)\\\equiv&\langle\chi_m|h_{mn}|\chi_n\rangle \ .\end{aligned} \tag{34}$$

A symmetric prescription in the hadronic expansion is necessary and sufficient to yield a Hermitian effective Hamiltonian. Without symmetrization, the extracted effective Hamiltonian need not be Hermitian for each level of truncation. The trouble is that the quark-model Hamiltonian is itself not self-adjoint in the restricted region $y\ge z$, or in the region $z\ge y$. Thus, "hadronization" with confined wave functions defined within these restricted regions is certain to be troubled; however, a symmetric prescription suffices to remedy the problem. Integration by parts with respect to y, in conjunction with Eq. (27) and the orthonormality condition for the φ_n's yields

$$\begin{aligned}h_{mn}^{(\mathrm{I})}(y)=&[-\partial_y^2+\varepsilon_n(y)]\delta_{nm}+\varphi_n(y;y)\partial_y\varphi_m(y;y)\\&+\int_0^y dz\{\partial_y\varphi_n(z;y)\partial_y\varphi_m(z;y)+\tfrac{1}{2}[\varphi_n(z;y)\partial_y^2\varphi_m(z;y)-\varphi_m(z;y)\partial_y^2\varphi_n(z;y)]\}\\&+\int_0^y dz[\varphi_n(z;y)\partial_y\varphi_m(z;y)-\varphi_m(z;y)\partial_y\varphi_n(z;y)]\vec{\partial}_y \ ,\end{aligned} \tag{35}$$

where the energy has been defined relative to $\varepsilon_0(\infty)=6$ and $\vec{\partial}_y$ acts to the right. Similarly, for scheme II, with Eq. (29),

$$\begin{aligned}h_{nm}^{(\mathrm{II})}(r)=&\left\{-\partial_r^2+\left[\varepsilon_n(r)-\varepsilon_0(\infty)-\frac{1}{2r^2}\right]\right\}\delta_{nm}\\&+\int_0^{\pi/4} r d\theta\left[4r^2(\sin^2\theta-\theta^2)\varphi_n\varphi_m+\partial_r\varphi_m\partial_r\varphi_n\right.\\&\left.+\frac{1}{2r}(\varphi_m\partial_r\varphi_n-\varphi_n\partial_r\varphi_m)+\tfrac{1}{2}(\varphi_m\partial_r^2\varphi_n-\varphi_n\partial_r^2\varphi_m)\right]+\int_0^{\pi/4} r d\theta(\varphi_m\partial_r\varphi_n-\varphi_n\partial_r\varphi_m)\vec{\partial}_r \ ,\end{aligned} \tag{36}$$

where the $\varphi_n(\theta;r)$ arguments have been suppressed and, as before, the energy is defined relative to $\varepsilon_0(\infty)=6$. Long-range effective forces apparently occur as a $1/(2r^2)$ term in the $n=m$ potentials; though, the r dependence of the φ_n's is not yet manifest.

To lowest order of truncation in either scheme, one finds a local effective Hamiltonian. Using the notation

$$h_{mn}(y)=-\partial_y^2+V_{mn}(y)\ ,$$

one has

$$V_{00}^{(\mathrm{I})}(y)=\varepsilon_0(y)-\varepsilon_0(\infty)+\varphi_0(y;y)\partial_y\varphi_0(y;y)+\int_0^y dz[\partial_y\varphi_0(z;y)]^2 \tag{37}$$

and

$$V_{00}^{(\mathrm{II})}(r)=\varepsilon_0(r)-\varepsilon_0(\infty)-\frac{1}{2r^2}+\int_0^{\pi/4} r\,d\theta[4r^2(\sin^2\theta-\theta^2)\varphi_0^2+(\partial_r\varphi_0)^2]\ . \tag{38}$$

The confined wave functions are calculated numerically via an expansion on a sine basis, chosen so as to become the exact eigenfunctions as the channel variable goes to zero. The final numerical results for V_{mn} through truncation $n=m=1$ are shown in Fig. 1. The channel potentials ($n=m$) are reminiscent of those found in meson-nucleon phenomenologies; they are of short range and exhibit a "hard-core" repulsion and intermediate-range attraction in the diagonal terms. $V_{00}(r)$ is qualitatively similar to $V_{00}(y)$; however, it is of much longer range, though the numerical falloff as $r\to\infty$ is not $O(r^{-2})$ as Eq. (37) naively indicates. V_{11} is similar in form to V_{00} in either scheme but has its minimum at larger r. This "pushing out" in r must be due, in part, to the larger hadron rms radius upon excitation.

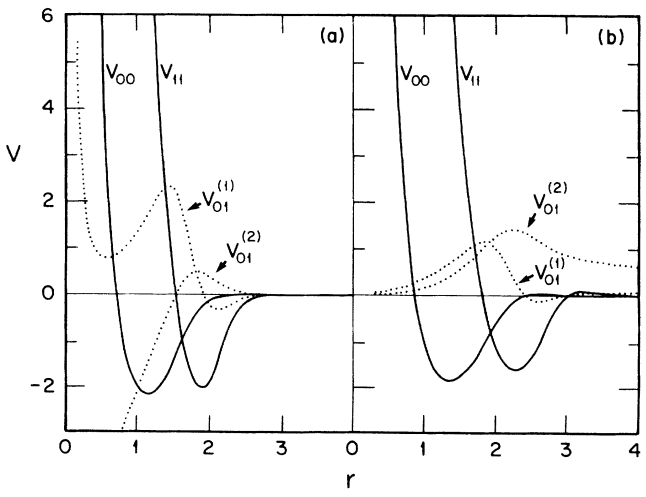

FIG. 1. Effective hadron potentials in U(1) color through $n=m=1$. The scale in r is set by $(\langle r^2\rangle)^{1/2}=\frac{1}{2}\sqrt{3}$, the isolated hadron ground-state radius, and in V by $\omega=4$. Here $V_{01}(y)=V_{01}^{(1)}(y)+V_{01}^{(2)}(y)\partial_y$. (a) (y,z) scheme [Eq. (35)], (b) (r,θ) scheme [Eq. (36).]

The stiff repulsion seen in $V_{00}(y)$ as $y\to 0$ and its attraction at large y follow from qualitative arguments. Consider the confined wave-function energy $\varepsilon_0(y)-\varepsilon_0(\infty)$, which dominates the behavior at small y and is still significant at large y. The imposition of the $\partial_z\varphi_0(z;y)|_{z=y}=0$ boundary condition will increase the curvature of the wave function relative to $\phi_0(z)$ at small y and, hence, $\varepsilon_0(y)>6$. For large y, the boundary condition lowers the curvature of the wave function so that $\varepsilon_0(y)<6$. The same argument follows for $\varepsilon_0(r)-\varepsilon_0(\infty)$, though the explicit $1/r^2$ term in scheme II's effective potentials and $\varphi_n(\theta;r)$'s dependence on r at large r makes any qualitative conclusion unclear.

Analytic limiting forms can be calculated in both schemes as the channel variable becomes very large or very small. In scheme I as $y\to 0$,

$$\varphi_n(z;y)\sim\sqrt{2/y}\sin\left[\frac{(2n+1)\pi z}{2y}\right]\ ,$$

so that

$$V_{00}\sim\left[\frac{\pi^2}{3}-\frac{3}{4}\right]\frac{1}{y^2}-6\ ,$$
$$V_{01}^{(1)}\sim\frac{1}{8y^2},\quad V_{10}^{(1)}\sim-\frac{19}{8y^2},\quad V_{01}^{(2)}\sim-\frac{5}{2y}\ , \tag{39}$$
$$V_{11}\sim(3\pi^2-\tfrac{3}{4})\frac{1}{y^2}-6\ .$$

Now in scheme II,

$$\varphi_n(\theta;r)\sim\sqrt{8/(\pi r)}\sin[2(2n+1)\theta]$$

as $r\to 0$. Thus,

$$V_{00}(r)\sim\frac{15}{4r^2}-6,\quad V_{11}(r)\sim\frac{143}{4r^2}-6\ , \tag{40}$$

so that $V_{11}(r)$ and $V_{11}(y)$ are much stiffer than $V_{00}(r)$ and $V_{00}(y)$ as the channel variable goes to zero, whereas $V_{01}^{(1)}(r)$ and $V_{01}^{(2)}(r)$ are finite in this limit. The $V_{10}^{(1)}$ limit is trivial in either scheme as, in general,

$$V_{10}^{(1)}=V_{01}^{(1)}-\partial_r V_{01}^{(2)}\ .$$

The formal solution for the $\varphi_n(z;y)$'s in scheme I for all y has the form

$$\varphi_n(z;y)=N_n(y)ze^{-z^2}\Phi\left[-\frac{\varepsilon_n(y)}{8}+\tfrac{3}{4},\tfrac{3}{2},2z^2\right]\ ,$$

where $\Phi(a,b,z)$ is a confluent hypergeometric function and $N_n(y)$ is a normalization to be determined. As $y\to\infty$, $-\varepsilon_n(y)/8+\frac{3}{4}\to -n$, so that $\Phi(a,b,z)$'s recursion relations in a and its $a\to 0$, large-z asymptotics can be used to yield an expression for $\varphi_n(z;y)$ for large z and y.[9] The boundary condition at $z=y$ yields $\varepsilon_n(y)$ at large y, and the normalization is calculated using the Wronskian of Eq. (27) and its y derivative. Now the integral $\int_0^y dz(\partial_y\phi_n)^2$ is peaked about $z=y$ for large y, so that an asymptotic series can be obtained, to yield, in leading order,

$$V_{00}(y)\sim -64\sqrt{2/\pi}y^3e^{-2y^2}\ ,$$
$$V_{11}(y)\sim 8-\frac{2^9}{3}\sqrt{2/3}y^7e^{-2y^2}\ . \tag{41}$$

The integrals in the off-diagonal terms are not surface peaked, so that the large-y forms of those potentials are not readily calculable.

The large-r behavior of all of scheme II's effective potentials can be calculated analytically upon the replacement $\varphi_n(\theta;r)\rightarrow\phi_n(r\theta)$. Unlike the previous (y,z) case, the asymptotic limits of the confined wave functions depend on the channel variable; this is an additional source of the long-range behavior of the potentials. As $r\rightarrow\infty$, then

$$\begin{aligned}
V_{00}&\sim\frac{7}{24r^4}+O(r^{-6})\ ,\\
V_{01}^{(1)}&\sim\frac{\sqrt{6}}{3r^2}+O(r^{-4})\ ,\\
V_{10}^{(1)}&\sim\frac{4\sqrt{6}}{3r^2}+O(r^{-4})\ ,\\
V_{01}^{(2)}&\sim\frac{\sqrt{6}}{r}\ ,\\
V_{11}&\sim\frac{21}{8r^4}+O(r^{-6})\ .
\end{aligned} \tag{42}$$

The large-r potential forms are not attractive; only terms in the potential that rely on the form of φ_n near $\theta=\pi/4$ in this symmetric case can be expected to be so. The $O(1/r^2)$ terms cancel identically for the diagonal potentials V_{00} and V_{11}, making them of shorter range than the channel couplings and supporting the numerical results shown in Fig. 1(b). The $V_{01}^{(2)}(r)$ calculation, except for an exponentially damped piece, is exact for large r. For the other results it is necessary to expand the $\sin^2\theta$ term in a power series in $1/r$; the order of the next higher term in the expansion is indicated.

The qualitative similarity of the $n=m$ potentials in schemes I and II is striking, though the observables in each scheme could very well turn out to be qualitatively different. The most marked difference between them at this point is the large-r behavior of the channel couplings; the power-law falloff of the couplings in scheme II is novel as such behavior was excluded from the underlying quark model by ansatz. These long-range potentials are unphysical: spin-independent hadron-hadron forces of range $O(r^{-5})$ or longer are ruled out by pionic atom data.[7] However, it is interesting to pursue the consequences of this scheme precisely because its behavior is qualitatively different from that of scheme I.

Low-energy scattering parameters were calculated in Ref. 1 for both of these schemes, and the binding energies with truncation were calculated as well. For scheme I,

$$\begin{aligned}
\varepsilon^{(0)}&=-0.0879\ ,\\
\varepsilon^{(1)}&=-0.118\ ,\\
\varepsilon^{(2)}&=-0.129\ ,
\end{aligned} \tag{43}$$

whereas, for scheme II,

$$\varepsilon_B^{(0)}=-0.108,\quad \varepsilon_B^{(1)}=-0.150\ . \tag{44}$$

The superscript denotes the truncation, and the quark-model binding energy is $\varepsilon_B=-0.160$. The large lowering of the energy in the (r,θ) case upon the addition of the next channel is a consequence of the long-range channel couplings and yields markedly good agreement with the quark-model binding energy. The stiffer repulsion of $V_{00}(r)$ as $r\rightarrow 0$ is manifested in a comparison of the effective ranges, and this stiffer repulsion yields poorer, though not poor, agreement with the quark-model phase shifts.

The binding energy with successive truncation in the (y,z) scheme does show convergence to the exact quark-model energy, even though it is not guaranteed to converge $\forall n,m$. This agreement is surprising as the hadronization scheme does not incorporate the exact quark-model boundary condition at $z=y$. The amount by which this hadronization violates the normal derivative constraint is

$$\partial_n\Psi(z,y)|_{z=y}=-\frac{1}{\sqrt{2}}\sum_n^{\sigma}[\partial_y\varphi_n(z;y)|_{z=y}\chi_n(y)+\varphi_n(y;y)\partial_y\chi_n(y)]\ , \tag{45}$$

where σ is the level of truncation in the hadronic expansion. This boundary function has been explicitly calculated for the $\sigma=2$ truncation. In comparison with the function

$$e^{-|\varepsilon_B^{(2)}|^{1/2}y}\phi_0(z)\ ,$$

which satisfies the Schrödinger equation, Eq. (11), in $y>z$ but no boundary condition at $z=y$, the $\sigma=2$ calculation shows no suppression of the normal derivative as calculated from Eq. (45). The observables which result from a few-channel truncation of this hadronic expansion are in good agreement with the quark-model observables and, in fact, become better and better representations of the observables studied with increasing truncation level; this is at odds with the size of the boundary function calculated and is not fully understood.

Before continuing, it is important to clarify the nature of the excitations included in a higher-order hadronic calculation. The excitations are in the reduced y,z basis, but the physical cluster states exist in the original $\mathbf{r}_i$ basis. A standard Moshinsky transformation connects the two bases, but the physical nature of a given y,z or r,θ excitation is not manifest.

B. Form factor

The bound-state form factor at high momentum transfer is a sensitive probe of short-range structure. As indicated in the beginning of Sec. III A, it is natural to calculate the hadronic form factor using both the effective wave functions and effective charge operators of a given scheme.

For scheme I, the effective charge operator may be constructed from the $P_n\hat{\rho}_qP_m$ prescription shown in Eq.

(25) in conjunction with Eq. (14b), in U(1) color. Rewriting this in terms of one-body and exchange pieces, one has

$$[\rho_q(y)]_{nm} \equiv [\rho_q^{\text{one-body}}(y)]_{nm} + [\rho_q^{\text{exch}}(y)]_{nm} , \tag{46a}$$

$$[\rho_q^{\text{one-body}}(y)]_{nm}^{(\text{I})} \equiv f_0(q) f_{nm}(q) j_0(qy/2) , \tag{46b}$$

$$[\rho_q^{\text{exch}}(y)]_{\text{nm}}^{(\text{I})} = f_{00}(q) j_0(qy/2) \times \left\{ \int_0^y dz [\varphi_n(z;y) j_0(qz/2) \varphi_m(z;y)] - f_{nm}(q) \right\} , \tag{46c}$$

where Eqs. (46b) and (46c) follow for $y > z$ and

$$f_{nm}(q) \equiv \int_0^\infty dz\, \phi_n(z) j_0\left[\frac{q}{2} z\right] \phi_m(z) .$$

$|f_{00}(q)|^2$ is the ground-state isolated hadron form factor. The one-body piece is defined so as to have a form-factor contribution identical to that of a convolution model. This form factor is merely a product of the "nuclear" form factor with pointlike hadrons and the internal hadron form factor. The exchange operator is what remains of the modified charge operator after the one-body piece is removed. The prescription for the one-body piece is now fixed, so that it has the same form for both projectors. Note that the exchange charge operator gives zero contribution as $q \to 0$ from charge conservation. Nor is there a contribution as $y \to \infty$ since the hadrons approach infinite separation. The resulting form-factor contributions are

$$F_{nm}^{\text{one-body}}(q) = \langle \chi_n^{(\sigma)} | (\rho_q^{\text{one-body}})_{nm} | \chi_m^{(\sigma)} \rangle , \tag{47a}$$

$$F_{nm}^{\text{exch}}(q) = \langle \chi_n^{(\sigma)} | (\rho_q^{\text{exch}})_{nm} | \chi_m^{(\sigma)} \rangle , \tag{47b}$$

with

$$F^{(\sigma)}(q) = \sum_{n,m}^{\sigma} [F_{nm}^{\text{one-body}}(q) + F_{nm}^{\text{exch}}(q)] . \tag{47c}$$

The channel wave functions $\chi_n^{(\sigma)}(y)$ depend on the original level of truncation σ. The form of Eq. (47) is clearly independent of the particular hadronization scheme.

For scheme II, the effective exchange charge operator is

$$[\rho_q^{\text{exch}}(r)]_{nm}^{(\text{II})} = f_{00}(q) \left\{ \int_0^{\pi/4} r d\theta \left[\varphi_n j_0\left[\frac{qr}{2}\cos\theta\right] j_0\left[\frac{qr}{2}\sin\theta\right] \varphi_m \right] - f_{nm}(q) j_0(qr/2) \right\} . \tag{48}$$

The $\varphi_n(\theta, r)$ arguments have been suppressed and $f_{nm}(q)$ is as above. Making the change of variable $z \equiv r\theta$, the limiting behavior of this operator at large r can be calculated via the replacement $\varphi_n(z/r; r) \to \phi_n(z)$, where the integration in the first term of Eq. (48) now extends to infinity, rather than to $r\pi/4$. This approximation has exponentially damped corrections in r. The resulting integral on $[0, \infty)$ is dominated by $z/r \ll 1$ for large r; expanding the j_0's in powers of z/r yields

$$[\rho_q^{\text{exch}}(r)]_{nm}^{(\text{II})} \sim -f_{00}(q) \frac{\cos(qr/2)}{2r^2} \int_0^\infty dz\, \phi_n(z) \phi_m(z) z^2 j_0\left[\frac{q}{2} z\right] + f_{00}(q) j_0\left[\frac{q}{2} r\right] \int_0^\infty dz\, \phi_n(z) \phi_m(z) \left[-\frac{z^2}{6r^2} \cos\left[\frac{q}{2} z\right] + j_0\left[\frac{q}{2} z\right] \left[\frac{2z^2}{3r^2} - \frac{q^2 z^4}{32 r^2}\right] \right] + O(r^{-4}) . \tag{49}$$

Since $\cos(qr/2)$, $\sin(qr/2) \sim 1$, the exchange charge operator has $O(1/r^2)$ behavior as $r \to \infty$; this justifies the neglect of the exponentially damped terms. If one now checks Eq. (49) in the limit of small q, the terms above vanish identically—as expected—with cancellation occurring between terms which are of different order in r, since $j_0(\xi) \to 1$ as $\xi \to 0$. To leading order,

$$[\rho_q^{\text{exch}}(r)]_{nm}^{(\text{II})} \sim -f_{00}(q) \frac{\cos(qr/2)}{2r^2} \times \int_0^{r\pi/4} dz\, \phi_n(z) \phi_m(z) z^2 j_0\left[\frac{q}{2} z\right] + O(r^{-3}) . \tag{50}$$

Doing the integral, the $n = m = 0$ operator has the form[10]

$$[\rho_q^{\text{exch}}(r)]_{00}^{(\text{II})} \sim -\frac{3}{8r^2}\left[1 - \frac{q^2}{48}\right] \cos\left[\frac{q}{2} r\right] \times e^{-q^2/32} + O(r^{-3}) . \tag{51}$$

This limiting behavior is in marked contrast to the exponentially damped numerical behavior of Eq. (46c) at large y.

The one-body and exchange form-factor contributions, Eq. (47), for both schemes were calculated in Ref. 1. Quantitative agreement with the quark-level form factor is seen in both schemes with only a two-channel truncation. The scale in q is set by the ground-state isolated hadron form factor, $|f_{00}(q)|^2 = e^{-q^2/16}$. The success persists even in extreme kinematic regimes; the form factor is well described by either hadronic basis with $\sigma = 1$ even when the isolated hadron form factor has fallen by 2 or-

ders of magnitude. Moreover, the $\sigma=2$ form-factor calculation in scheme I is a still better description of the quark-level form factor; this is surprising because an explicit calculation of the $\sigma=2$ boundary function in this scheme shows that it is not "small," that is, in comparison to the normal derivative of

$$e^{-|\varepsilon_B^{(2)}|^{1/2}y}\phi_0(z) .$$

Yet, the significance of this in relation to the form-factor convergence is unclear; a calculation of the $\sigma=0$ and $\sigma=1$ boundary functions is lacking. A sensitive cancellation of the one-body and exchange contributions in each scheme gives rise to the convergence seen. The insensitivity of the results thus far to the particular hadronic scheme is remarkable; the two hadronization schemes are qualitatively different. This is manifested not only in the long-range behavior of their effective potentials but also in their effective charge operators.

C. Momentum distribution

The quark-level momentum distribution is qualitatively different from the other observables so far considered in that its "softening," that is, its enhancement at low p, cannot be reproduced in any inert meson description. In the discussion that follows, low and high p shall refer to $p \ll \langle p^2\rangle^{1/2}$ and $p \gg \langle p^2\rangle^{1/2}$, respectively. The momentum distribution of a particular hadronic state in either scheme may be calculated using Eqs. (16) and (17). Inserting hadronic projectors, such as Eq. (30) or (31), yields $[n(p)]_{nm}$ for any level of truncation. This is certainly tractable, but it is far easier to calculate the second moment of the momentum distribution instead. This observable, like the momentum distribution itself, is qualitatively distinct from what could be obtained in any inert meson description. That is, $\langle p^2\rangle_{\text{quark}}$ is less than $\frac{3}{2}$, the isolated hadron second moment; any package model can yield only an increase.

The calculation of the second moment of the momentum distribution proceeds in a manner analogous to the calculation of $\langle p^2\rangle_{\text{quark}}$. Consider the commutator of the dilatation operator with the Hamiltonian

$$\langle\Psi|[\mathbf{x}\cdot\mathbf{p}_{(x)}+\mathbf{y}\cdot\mathbf{p}_{(y)}+\mathbf{z}\cdot\mathbf{p}_{(z)},H]|\Psi\rangle ,$$

now, however, the state $|\Psi\rangle$ is no longer the exact $q^2\bar{q}^2$ bound state but, rather, a hadronic wave function calculated in a truncated basis of hadron internal excited states. Thus, this expression is no longer identically zero; the virial theorem does not necessarily hold in the hadronic basis. The $\langle p^2\rangle$ is calculated in the following way. The hadronic wave function at some truncation σ is used to compute the expectation value of the commutator above. This result is related to $\langle p^2\rangle$ by using Eqs. (18) and (19) while noting that, for hadronic wave function $|\Psi\rangle$, the right-hand side of Eq. (18) is now evaluated using the hadronic wave function's binding energy.

In scheme I, $|\Psi\rangle$ becomes

$$|\Psi\rangle=\frac{1}{\sqrt{4\pi x}}\phi_0(x)\frac{1}{4\pi yz}\Psi_B^{(\mathrm{I})}(z,y) , \tag{52}$$

where $\Psi_B^{(\mathrm{I})}$ is given by Eq. (32) with the sum terminated at level σ. Using Eq. (6) in U(1) color with s waves only, gives

$$\langle\Psi|[\mathbf{x}\cdot\mathbf{p}_{(x)}+\mathbf{y}\cdot\mathbf{p}_{(y)}+\mathbf{z}\cdot\mathbf{p}_{(z)},H]|\Psi\rangle$$
$$=-2i\sum_{n,m}^{\sigma}\int_0^\infty dy\int_0^y dz\,\varphi_n(z;y)\chi_n(y)\{y[\partial_y\varepsilon_m(y)]+2\partial_y^2+[\varepsilon_m(y)-\varepsilon_n(y)](z\partial_z+y\partial_y)\}\varphi_m(z;y)\chi_m(y) . \tag{53}$$

"Symmetrizing" this expression in n,m should eventually yield an expression similar to the effective Hamiltonian. After this and use of Eq. (27) and the $\varphi_n(z;y)$ orthonormality relations, one finds

$$\langle\Psi|[\mathbf{x}\cdot\mathbf{p}_{(x)}+\mathbf{y}\cdot\mathbf{p}_{(y)}+\mathbf{z}\cdot\mathbf{p}_{(z)},H]|\Psi\rangle=2i\sum_{n,m}^{\sigma}\int_0^\infty dy\,\chi_n(y)\left\{h_{nm}^{(\mathrm{I})}(y)+\delta_{nm}[-\tfrac{1}{2}y\partial_y\varepsilon_n(y)-\varepsilon_n(y)]-\frac{\varepsilon_m(y)-\varepsilon_n(y)}{2}\right.$$
$$\left.\times\int_0^y dz\,\varphi_n(z;y)(z\partial_z+y\partial_y)\varphi_m(z;y)\right\}\chi_m(y) . \tag{54}$$

Using Eq. (19) and the right-hand side of Eq. (18), where ε_B is now the binding energy of the hadronic wave function to a given level of truncation, $\varepsilon_B^{(\sigma)}$, one finds that Eq. (54) equals $2i\{8\langle p^2\rangle-(12+\varepsilon_B^{(\sigma)})\}$, so that $\langle p^2\rangle_{(\sigma)}^{(\mathrm{I})}$ is

$$\langle p^2\rangle_{(\sigma)}^{(\mathrm{I})}=\tfrac{3}{2}+\tfrac{1}{4}\varepsilon_B^{(\sigma)}-\tfrac{1}{8}\sum_{n,m}^{\sigma}\int_0^\infty dy\,\chi_n(y)\left[\delta_{nm}\{\tfrac{1}{2}y\partial_y\varepsilon_n(y)+[\varepsilon_n(y)-6]\}\right.$$
$$\left.+\frac{\varepsilon_m(y)-\varepsilon_n(y)}{2}\int_0^y dz\,\varphi_n(z;y)(z\partial_z+y\partial_y)\varphi_m(z;y)\right]\chi_m(y) , \tag{55}$$

where $\varepsilon_0(\infty)=6$. For $\sigma=0$,

$$\langle p^2\rangle_{(0)}^{(\mathrm{I})}=\tfrac{3}{2}+\tfrac{1}{4}\varepsilon_B^{(0)}-\tfrac{1}{8}\int_0^\infty dy\,\chi_0^2(y)\{\tfrac{1}{2}y\partial_y\varepsilon_0(y)+[\varepsilon_0(y)-6]\} . \tag{56}$$

To analyze the sign of the integral in Eq. (56), consider that, as $y\to 0$,

$$\varepsilon_n(y)\sim\left[\frac{(2n+1)\pi}{2y}\right]^2,\quad \frac{y}{2}\partial_y\varepsilon_n(y)\sim-\varepsilon_n(y)\ . \tag{57}$$

However, for large y, the asymptotics of $\varphi_0(z;y)$ for large z and y yield

$$\varepsilon_0(y)-6\sim-32\sqrt{2/\pi}y^3e^{-2y^2} \tag{58}$$

in leading order, so that $\varepsilon_0(y)-6<0$ and $\frac{1}{2}y\partial_y\varepsilon_0(y)>0$ at large y. Thus, even though $\varepsilon_B^{(0)}$ is clearly less than zero, the overall sign of the terms which add to the isolated meson result of $\frac{3}{2}$ is not manifest. An explicit numerical calculation yields

$$\langle p^2\rangle_{(0)}^{(\mathrm{I})}=1.4855\ ,\quad \langle p^2\rangle_{(1)}^{(\mathrm{I})}=1.4836,\quad \langle p^2\rangle_{(2)}^{(\mathrm{I})}=1.4833\ , \tag{59}$$

where $\langle p^2\rangle_{\text{quark}}=1.4800$. This hadronic scheme seems quite successful: the second moment of the lowest truncation is less than the isolated meson result—in contrast to an inert meson description—and the $\langle p^2\rangle$ of successive truncations seems to converge, albeit slowly, to the quark-model result.

For scheme II, replacing $\Psi_B^{(\mathrm{I})}(z,y)$ in Eq. (18) with $\Psi_B^{(\mathrm{II})}(r,\theta)$, Eq. (33), finally yields, after "symmetrization" and use of Eqs. (28) and (29),

$$\langle p^2\rangle_{(\sigma)}^{(\mathrm{II})}=\tfrac{3}{2}+\tfrac{1}{4}\varepsilon_B^{(\sigma)}-\tfrac{1}{8}\sum_{n,m}^{\sigma}\int_0^\infty dr\,\chi_n(r)\left[\delta_{nm}\left\{\frac{r}{2}\partial_r\varepsilon_m(r)+[\varepsilon_m(r)-6]\right\}+8r^2\int_0^{\pi/4}rd\theta\,\varphi_n(\sin^2\theta-\theta^2)\varphi_m\right.$$
$$\left.+\frac{r}{2}[\varepsilon_m(r)-\varepsilon_n(r)]\int_0^{\pi/4}rd\theta\,\varphi_n\partial_r\varphi_m\right]\chi_m(r)\ , \tag{60}$$

where $\varepsilon_0(\infty)=6$ and $\varphi_n\equiv\varphi_n(\theta;r)$. To lowest order in truncation,

$$\langle p^2\rangle_{(0)}^{(\mathrm{II})}=\tfrac{3}{2}+\tfrac{1}{4}\varepsilon_B^{(0)}-\tfrac{1}{8}\int_0^\infty dr\,\chi_0^2(r)\left\{\frac{r}{2}\partial_r\varepsilon_0(r)+[\varepsilon_0(r)-6]+8r^2\int_0^{\pi/4}rd\theta\,\varphi_0^2(\sin^2\theta-\theta^2)\right\}\ . \tag{61}$$

Now, for small r,

$$\varepsilon_n(r)\sim\left[\frac{2(2n+1)}{r}\right]^2,\quad \frac{r}{2}\partial_r\varepsilon_n(r)\sim-\varepsilon_n(r)\ , \tag{62}$$

$$r^2\int_0^{\pi/4}rd\theta\,\varphi_0^2(\sin^2\theta-\theta^2)\sim\left[\frac{3}{4}-\frac{2}{3\pi}-\frac{\pi^2}{48}\right]r^2<0\ .$$

For large r, $\varepsilon_n(r)-6$ is identical in form to Eq. (58) with $r\pi/4\equiv y$ and, thus, it and $\frac{1}{2}r\partial_r\varepsilon_0(r)$ are exponentially damped in this limit. However, the $\sin^2$ term has the form

$$r^2\int_0^{\pi/4}rd\theta\,\varphi_0^2(\sin^2\theta-\theta^2)\sim-\frac{5}{16r^2}+\frac{7}{96r^4}+O(r^{-6}) \tag{63}$$

so that it is of long range and ultimately gives a positive contribution to Eq. (61). Numerical calculation shows the $\sin^2$ term of Eq. (63) to be negative definite for all r, thus giving a large positive contribution to $\langle p^2\rangle_{(0)}$. An explicit computation of $\langle p^2\rangle_{(\sigma)}^{(\mathrm{II})}$ yields

$$\langle p^2\rangle_{(0)}^{(\mathrm{II})}=1.5498,\quad \langle p^2\rangle_{(1)}^{(\mathrm{II})}=1.4882\ . \tag{64}$$

The $\sigma=0$ moment is greater than the isolated meson value; it gains a contribution of $+0.0545$ from the $\sin^2$ term mentioned above. This large value can be traced to the power-law falloff of the $\sin^2$ term at large r, which, in turn, is related to the definition of the confined wave functions, Eq. (29), and the long-range behavior of the effective forces. However, it is not the choice of the confined wave functions which causes this result to go astray. It would have been possible to define confined wave functions $\eta_n(\theta;r)$ such that

$$\left[-\frac{1}{r^2}\partial_\theta^2+4r^2\sin^2\theta\right]\eta_n(\theta;r)=\varepsilon_n(r)\eta_n(\theta;r)\ . \tag{65}$$

If one were now to calculate the $\langle p^2\rangle$ in a scheme with these confined wave functions, the objectionable $\sin^2$ term above would no longer exist. However, $\eta_n(\theta;r)$ approaches $\phi_n(r\theta)$ as $r\to\infty$ with power-law corrections, so that it is now the term

$$\frac{r}{2}\partial_r\varepsilon_0(r)+[\varepsilon_0(r)-6]$$

which has power-law falloff and gives a large positive contribution to $\langle p^2\rangle_{(0)}$. That is, for large r,

$$4r^2\sin^2(z/r)\sim4z^2-\frac{4z^4}{3r^2}+\frac{8z^6}{45r^4}+O(r^{-6})\ ,$$

where $z\equiv r\theta$. In this limit, then,

$$\frac{r}{2}\partial_r\varepsilon_0(r)+[\varepsilon_0(r)-6]$$
$$\sim-\frac{8}{45r^4}\langle\phi_0|z^6|\phi_0\rangle-\frac{16}{9r^4}\sum_{m\neq0}\frac{|\langle\phi_m|z^4|\phi_0\rangle|^2}{\varepsilon_m-\varepsilon_0}\ ,$$

and the resulting contribution to $\langle p^2\rangle_{(0)}$ is positive. This is not conclusive; however, it seems to indicate that the $\langle p^2\rangle_{(0)}^{(II)} > \frac{3}{2}$ result is more a consequence of the original choice of confined coordinates than of the choice of the confined wave functions themselves.

In conclusion, the confinement scheme which generated good agreement in the lowest order of truncation to the other U(1) observables studied is in qualitative disagreement with the quark model $\langle p^2\rangle$ to the same order. However, the sign of $\langle p^2\rangle - \frac{3}{2}$ does not necessarily determine the behavior of the momentum distribution relative to $n_{\rm isol}(p)$ at low p. If $\langle p^2\rangle < \frac{3}{2}$, then this constraint plus the normalization condition $\int d^3p\, n(\mathbf{p}) = 1$ and the Fermi motion constraint $n(p) > n_{\rm isol}(p)$ at large p does imply that the momentum distribution must be softer at low p than the isolated meson case. However, if $\langle p^2\rangle > \frac{3}{2}$, the enhancement of $n(p)$ at low p is no longer guaranteed, though it may exist. The $\sigma = 0$ scheme-II wave function may build in some of the correct behavior at low p because the $\sigma = 1$ result is markedly improved, even though it is certainly still worse than the lowest-order scheme-I result.

Both effective schemes considered are able to reproduce the softening of the quark-momentum distribution seen at low p upon inclusion of a single excited hadron internal state. At the $\sigma = 0$ level, scheme I is already able to reproduce the $\langle p^2\rangle < \frac{3}{2}$ result and, thus, assuredly has the qualitative low-p behavior of the true momentum distribution. This is marked as an inert meson description is wholly unable to reproduce the $\langle p^2\rangle < \frac{3}{2}$ result and, indeed, cannot reproduce the softening of $n(p)$ seen here with the inert meson states $\phi_n(z)$ of this model without the explicit inclusion of excited hadron internal states.[2]

IV. SU(N) HADRONIZATION

I shall now construct effective hadronic theories from the SU(N) quark model, which is governed by the Hamiltonian, Eq. (12). Equation (12) is a set of differential equations in Ψ_0 and Ψ_1 that are coupled by virtue of the boundary condition on the rearrangement surface, $z = y$. The SU(N) Ψ_0 only differs from its U(1) counterpart by virtue of this boundary condition, Eq. (13). Equation (13) can be rewritten as

$$\left.\frac{\partial_n \Psi_0(y,z)}{\Psi_0(y,z)}\right|_{z=y=t} = -\frac{1}{\lambda}\left.\frac{\partial_n \Psi_1(y,z)}{\Psi_1(y,z)}\right|_{z=y=t}, \tag{66}$$

where $\lambda \equiv (N+s)/(N-s)$. The size of the coupling to the hidden color sector is clearly dialed by N and s, the overall symmetry of the wave function; thus, λ provides a useful parametrization between the antisymmetric U(1) ($\lambda = 0$) and symmetric U(1) ($\lambda = \infty$) limits. I will continue to consider the overall symmetric state, $s = 1$, and I shall choose $q^2\bar{q}^2$ systems with ν_c and λ such that a bound state exists. Such choices with $\nu_c \gtrsim 0.5$ are the most sensitive to the presence of the hidden color sector, as indicated by the SU(N) phase shifts. Thus, $\nu_c = 0.5$, $\lambda = 3$; $\nu_c = 0.6$, $\lambda = 3$; and $\nu_c = 0.6$, $\lambda = 2$ systems are considered. $\lambda = 3$ corresponds to the internal color group SU(2), and $\lambda = 2$ corresponds to SU(3). Since the normal derivative of the wave function at $y = z$ is finite and yet the wave function is symmetric, this means that the normal derivative will vary in sign upon calculation above or below the rearrangement surface.

Any of the schemes discussed in the U(1) section can, in principle, be used in the SU(N) case as well. The convergence to the "wrong" results would be evident, though, even after the inclusion of the first excited hadron internal state; the energies of the $\sigma = 1$ U(1) schemes discussed are overbound with respect to the quark-model energies of the $\nu_c = 0.6$, $\lambda = 3$ and $\nu_c = 0.6$, $\lambda = 2$ systems. Incorporation of the SU(N) boundary condition, Eq. (66), in any hadronization scheme constructed is thus crucial in yielding convergence to the SU(N) results. It seems cogent to concentrate on hadronic schemes in which the confined coordinate becomes the normal coordinate at $z = y$: the importance of the $z = y$ boundary condition dictates that the exact quark-level boundary condition be embedded in the confined wave function's behavior at the rearrangement surface. That is, I shall consider coordinates (r,ξ) such that the confined wave function $\varphi_n(\xi;r)$ satisfies

$$\partial_\xi \varphi_n(\xi;r)|_{\xi=\xi(r)} = \tilde{g}(r)\varphi_n(\xi;r), \tag{67}$$

where $\xi = \xi(r)$ specifies the rearrangement surface. The novel departure is the $\tilde{g}(r)$ term. This function contains the boundary condition information of the quark model

$$\tilde{g}(t) \equiv \left.\frac{(\partial_z - \partial_y)\Psi_0(y,z)}{\Psi_0(y,z)}\right|_{z=y=t} \tag{68}$$

and will be used as input to the hadronization calculations of this section. The $\tilde{g}(r)$'s for the systems considered are shown in Fig. 2. They are calculated from the quark model Ψ_0 and $\partial_n \Psi_0$ on $z = y = t$, which are, in turn, calculated using the $\phi_n^{l=1}(t)$ expansion results of Rosenfelder.[11] The use of the $\tilde{g}(r)$'s is no departure from the philosophy of the previous section; these boundary functions are not free parameters but, rather, are fully specified by the physics of the quark model. Thus, this procedure is identical in spirit to the U(1) schemes in which merely a zero normal derivative constraint was embedded in the hadronization.

I shall consider the following two hadronization schemes. First, a (r,θ) scheme with r and θ as before ($z = r\sin\theta$, $y = r\cos\theta$) will be discussed. Despite the unsatisfactory long-range pieces in the polar Laplacian, this scheme can incorporate Eq. (67) exactly. The use of this scheme, though, is hardly a compromise. At the U(1) level, the agreement to the quark-model observables after including merely one excited hadron internal state is impressive. Second, I shall compare the more extensive results of the (r,θ) scheme with a (z,y) scheme similar to the U(1) case in which $\partial_z \varphi_n(z;y)$ at $z = y = t$ is now constrained to be $\tilde{g}(t)\varphi_n(z;y)$. This last is merely an attempt to gauge the sensitivity of the hadronization to the form of the boundary condition incorporating $\tilde{g}(r)$.

The confined wave functions shall be chosen to satisfy the same equations of motion and orthogonality relations as in the U(1) case. [See Eq. (29).] Now, however, the $\varphi_n(\theta;r)$ satisfy

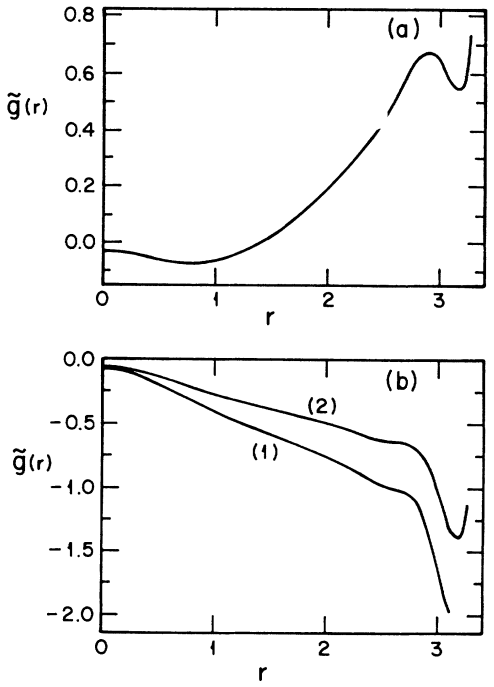

FIG. 2. The SU(N) quark-level boundary function $\tilde{g}(r)$ vs r [see Eq. (67)]. In this model, the choice of λ and ν_c completely determine the hidden color dynamics. ν_c specifies the physical extent of the color nonsinglet sector relative to the color singlet one, whereas $\lambda=(N+s)/(N-s)$ specifies the strength of the coupling of the two sectors. N is the number of colors, and s is the symmetry of the state under quark exchange—here, and in what follows, only the symmetric state ($s=1$) will be considered [see Eqs. (10) and (66)]. (a) $\nu_c=0.5$. $\lambda=3$. (b) (1) is $\nu_c=0.6$, $\lambda=3$, and (2) is $\nu_c=0.6$, $\lambda=2$.

$$\left.\frac{\partial_\theta\varphi_n(\theta;r)}{\varphi_n(\theta;r)}\right|_{\theta=\pi/4}=\frac{r}{\sqrt{2}}\tilde{g}\left[\frac{r}{\sqrt{2}}\right] . \tag{69}$$

The additional r and $\sqrt{2}$ factors come from the mapping to polar coordinates. That is, $(\sqrt{2}/r)\partial_\theta\equiv\partial_z-\partial_y$ and $z=y=t=r/\sqrt{2}$. The expansion

$$\varphi_n(\theta;r)=\sum_{m=1} A_m^{(n)}(r)\sin(2b_m\theta)$$

is used as in the U(1) case. Requiring that the sine expansion for φ_n satisfies the boundary condition of Eq. (69) term by term yields a transcendental equation for the b_m

$$\frac{b_m\pi}{2}\cot\left[\frac{b_m\pi}{2}\right]=\frac{r\pi}{4\sqrt{2}}\tilde{g}\left[\frac{r}{\sqrt{2}}\right] . \tag{70}$$

A coefficient $c_m\equiv b_m\pi/2$ must be generated in each $[(m-1)\pi,m\pi]$ interval. A solution c_m clearly exists for any $m>1$ and is readily generated using the Newton-Raphson method. There is no solution, however, for $m=1$ if the right-hand side of Eq. (70) is larger than 1. "Losing" the nodeless term in the sine expansion has disastrous consequences on the convergence of the sine expansion itself. The sign of $\tilde{g}(r/\sqrt{2})$ for the various cases are such that this failure could occur only for the $\nu_c=0.5$, $\lambda=3$ case. Luckily, the factors of $\sqrt{2}$ and the specific form of $\tilde{g}(r/\sqrt{2})$ conspire to allow a calculation of the c_m's through $r\approx4$, which should suffice for a numerical calculation of the effective potentials. Note that $r=4$ corresponds to evaluating $\tilde{g}(t)$ at ≈2.8, so that the obvious instability in the quark-boundary-function ratio is avoided. The instability in this ratio certainly does not seem to affect the results found: the effective potentials of the (r,θ) schemes with varying ν_c and λ calculated at $r=4$ all agree well with the large-r analytic forms.

The derivation of the effective Hamiltonian now follows as before. The projector has the same form, Eq. (31), and, consequently, a symmetric prescription for the energy yields an expression for $h_{nm}(r)$ *identical* in form to that of the U(1) case. [See Eq. (36).] The effective potentials are, of course, numerically distinct from the U(1) case, since the confined wave functions satisfy different boundary conditions. However, the large-r behavior of the effective potentials is precisely as in the U(1) case, Eq. (42). The long-range behavior comes from the confined wave function's mapping to an isolated hadron spectrum $\phi_n(r\theta)$ that depends on r and not from any details of the confined wave function's boundary condition at $\theta=\pi/4$. Thus, the striking long-range channel couplings seen in the U(1) case are preserved here as well. The Gaussian damped pieces will depend on the boundary condition; note

$$\varepsilon_0(r)-\varepsilon_0(\infty)\sim-32\sqrt{2/\pi}\left[\frac{r\pi}{4}\right]^3 e^{-2(r\pi/4)^2}\times\left[1+2\sqrt{2}\tilde{g}\left[\frac{r}{\sqrt{2}}\right]\frac{1}{r\pi}+O(r^{-2})\right] . \tag{71}$$

These terms, though, are clearly irrelevant for sufficiently large r. The $r\to0$ behavior for the V_{00}, V_{11} potentials is as in the U(1) case, Eq. (40). For small r, the sine functions are independent of r since Eq. (70) becomes identical to the U(1) case as $r\to0$; the $O(1/r^2)$ behavior comes from their normalization.

Consider now the derivation of the effective charge operator for the SU(N) case. The total quark-level form factor has both Ψ_0 and Ψ_1 contributions:

$$F(q)=2e^{-q^2/32}\times\int_0^\infty dy\int_0^y dz\, j_0\left[\frac{q}{2}y\right]j_0\left[\frac{q}{2}z\right]\times[\Psi_0^2(y,z)+\Psi_1^2(y,z)] . \tag{72}$$

A hadronization of the Ψ_0 piece of the form factor yields an effective charge operator identical in form to that found previously. The convolution model form factor of this singlet piece is identical to that of the U(1) case, so that pulling out the one-body piece yields

$$[\rho_0^{\rm exch}(r)]_{\rm nm}=f_{00}(q)\left\{\int_0^{\pi/4}rd\theta\left[\varphi_n j_0\left[\frac{qr}{2}\cos\theta\right]j_0\left[\frac{qr}{2}\sin\theta\right]\varphi_m\right]-f_{nm}(q)j_0(qr/2)\right\}. \tag{73}$$

Equation (73) has the same $r\to\infty$ and $r\to 0$ behavior as the U(1) exchange charge operator since the calculation of these limiting forms does not depend on the detailed form of the confined wave functions at $\theta=\pi/4$. [See Eq. (50).] The SU(N) color singlet exchange charge operator is thus of $O(1/r^2)$ for large r. Additional contributions to the effective charge operator above come from the hidden color sector $\Psi_1(y,z)$. The hidden color portion of the form factor defines the nonlocal hidden color charge operator $\rho_{nm}^{\rm hc}(r',r'')$, that is,

$$\begin{aligned}F_{\rm hc}(q)&=2e^{-q^2/32}\int_0^\infty dy\int_0^y dz\, j_0\left[\frac{q}{2}y\right]j_0\left[\frac{q}{2}z\right]\Psi_1^2(y,z)\\&\equiv\sum_{n,m}\int_0^\infty dr'\int_0^\infty dr''\chi_n(r')\rho_{nm}^{\rm hc}(r',r'')\chi_m(r''),\end{aligned} \tag{74}$$

where $\chi_n(r)$ is a color singlet channel wave function. To extract $\rho_{nm}^{\rm hc}(r',r'')$, consider Green's theorem for $\Psi_1(y,z)$ in terms of Ψ_1 and $\partial_n\Psi_1$ on the $z=y$ boundary. Using the boundary conditions, Eq. (13), to replace the Ψ_1 values there yields

$$\Psi_1(y,z)=\frac{1}{\beta}\int_0^\infty dt'[G_1(y,z,t',t')(\alpha+s)\partial_n\Psi_0(t',t')-(\alpha-s)\Psi_0(t',t')\Gamma_1(y,z,t',t')], \tag{75}$$

where $\Gamma_1(y,z,t',t')\equiv(\partial_{z'}-\partial_{y'})G_1(y,z,y',z')|_{z'=y'=t'}$ and $G_1(y,z,y',z')$ is the hidden color Green's function defined by

$$[\varepsilon-h_1(y,z)]G_1(y,z,y',z')=\delta(y-y')\delta(z-z').$$

The hadronic expansion of Ψ_0 and $\partial_n\Psi_0$, Eqs. (33) and (69), for $\theta=\pi/4$ yields

$$\Psi_0(\theta,r)\Big|_{\theta=\pi/4}=\frac{1}{\sqrt{2}}\sum_n\varphi_n(\pi/4;r)\chi_n(r), \tag{76a}$$

$$\partial_\theta\Psi_0(\theta,r)\Big|_{\theta=\pi/4}=\frac{r}{2}\tilde{g}\left[\frac{r}{\sqrt{2}}\right]\sum_n\varphi_n(\pi/4;r)\chi_n(r). \tag{76b}$$

Using the above and Eq. (75) in Eq. (74) gives, finally,

$$\begin{aligned}\rho_{nm}^{\rm hc}(r',r'')=\frac{e^{-q^2/32}}{\beta^2}\Bigg[&\frac{r'}{\sqrt{2}}\tilde{g}\left[\frac{r'}{\sqrt{2}}\right]\varphi_n(\pi/4;r')\tilde{\alpha}(r',r'')(\alpha+s)^2\frac{r''}{\sqrt{2}}g\left[\frac{r''}{\sqrt{2}}\right]\varphi_m(\pi/4;r'')\\&-(\alpha^2-1)\varphi_n(\pi/4;r')\tilde{\beta}(r',r'')\frac{r''}{\sqrt{2}}g\left[\frac{r''}{\sqrt{2}}\right]\varphi_m(\pi/4;r'')\\&-(\alpha^2-1)\frac{r'}{\sqrt{2}}g\left[\frac{r'}{\sqrt{2}}\right]\varphi_n(\pi/4;r')\tilde{\beta}(r'',r')\varphi_m(\pi/4;r'')\\&+(\alpha-s)^2\tilde{\gamma}(r',r'')\varphi_n(\pi/4;r')\varphi_m(\pi/4;r'')\Bigg],\end{aligned} \tag{77}$$

where $\tilde{\alpha}$, $\tilde{\beta}$, and $\tilde{\gamma}$ contain the integrals over the hidden color Green's function and its normal derivative. Specifically,

$$\int_0^\infty dr\int_0^{\pi/4}rd\theta\, j_0\left[\frac{q}{2}\tilde{y}\right]j_0\left[\frac{q}{2}\tilde{z}\right]G_I(\tilde{y},\tilde{z},r',r')G_I(\tilde{y},\tilde{z},r'',r'')\equiv\tilde{\alpha}(r',r''), \tag{78a}$$

$$\int_0^\infty dr\int_0^{\pi/4}rd\theta\, j_0\left[\frac{q}{2}\tilde{y}\right]j_0\left[\frac{q}{2}\tilde{z}\right]G_I(\tilde{y},\tilde{z},r'',r'')\Gamma_I(\tilde{y},\tilde{z},r',r')\equiv\tilde{\beta}(r',r''), \tag{78b}$$

$$\int_0^\infty dr\int_0^{\pi/4}rd\theta\, j_0\left[\frac{q}{2}\tilde{y}\right]j_0\left[\frac{q}{2}\tilde{z}\right]\Gamma_I(\tilde{y},\tilde{z},r',r')\Gamma_I(\tilde{y},\tilde{z},r'',r'')\equiv\tilde{\gamma}(r',r''), \tag{78c}$$

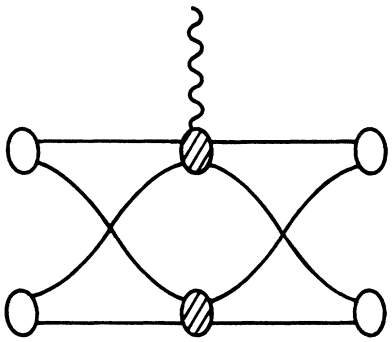

FIG. 3. Schematic illustration of the hidden color contribution to the effective form factor. Two color singlet hadrons upon quark exchange have some probability of being in a hidden color state, as indicated by the shaded portion of the figure. The photon may couple to either the color singlet or hidden color states; the hidden color state's contribution to the wave-function normalization yields a finite contribution at $q=0$.

with $\tilde{z}=r\sin\theta$, $\tilde{y}=r\cos\theta$. $\rho^{\rm hc}_{nm}(r',r'')$ is not purely an exchange operator; it is finite at $q=0$. A schematic picture of the processes included in $\rho^{\rm hc}_{nm}(r',r'')$ is shown in Fig. 3. There are hidden color contributions to both the U(1) one-body and exchange contributions, and the former is responsible for the nonvanishing contribution at $q=0$. The hidden color piece therefore contributes to the normalization of $\chi_n(r)$. At the hadronic level, though, the channel wave-function normalization is determined by the usual hadronic constraint $\sum_n \int_0^\infty dr\,\chi_n^2(r)=1$. It is more reasonable, then, to think of the constant adjustment to the form factor for all q as a "dressing" of the elementary charge of the hadrons. The calculation of $\rho^{\rm hc}_{nm}(r,r')$ is rather complicated, so that convergence to merely the Ψ_0 piece of the form factor has been considered. This separation of the total form factor into singlet and hidden color components is artificial, but in the context of the model it is completely unambiguous. Convergence to the singlet form factor is necessary for the hadronic scheme to be sensible, though it is not a sufficient requirement since the convergence to the hidden color component may be different.

The effective potentials through $n=m=1$ of the (r,θ) effective Hamiltonian have been calculated for the $\nu_c=0.5$, $\lambda=3$; $\nu_c=0.6$, $\lambda=3$; and $\nu_c=0.6$, $\lambda=2$ cases. As per the earlier discussion, the large-r behavior of all the potentials is the same. The small-r behavior of the channel potentials ($n=m$) is certainly the same. The differences between the $\varphi_n(\theta;r)$ for various (ν_c,λ) are manifested in the intermediate regions of the potentials and mainly in the diagonal terms, in the sizes of the potential minima and in the extent in r of the wells. The potentials all look rather similar, and thus only the potentials of the $\nu_c=0.5$, $\lambda=3$ and $\nu_c=0.6$, $\lambda=2$ systems are plotted in Fig. 4. The depths of the wells in the respective cases reflect the binding energies of the original quark systems: $\varepsilon_B(\nu_c=0.5,\ \lambda=3)<\varepsilon_B(\nu_c=0.6,\ \lambda=3)<\varepsilon_B(\nu_c=0.6,\ \lambda=2)$. These differences are also manifest in a calculation of the scattering lengths in $\sigma=0$. That is, direct integration of the respective V_{00}'s yield $a(\nu_c=0.5,\ \lambda=3)=4.58$, $a(\nu_c=0.6,\ \lambda=3)=6.28$, and $a(\nu_c=0.6,\ \lambda=2)=8.46$. These scattering lengths are somewhat less attractive than the scattering lengths in the respective quark models, and are certainly less attractive than the U(1) (r,θ) $\sigma=0$ scattering length $a=4.27$.[1,2]

The binding energies of the $\nu_c=0.5$, $\lambda=3$ system with truncation are $\varepsilon_B^{(0)}=-8.89\times10^{-2}$ and $\varepsilon_B^{(1)}=-0.129$. The energy of the $\sigma=1$ truncation is in good agreement with the quark-model energy $\varepsilon_q=-0.140$.[2] Numerical calculations indicate that the $\nu_c=0.6$, $\lambda=3$ and $\nu_c=0.6$, $\lambda=2$ systems are bound as well. The $\sigma=0$ and $\sigma=1$ form factors of the $\nu_c=0.5$, $\lambda=3$ system have been calculated using the above binding energies. [See Eqs. (47), (73), and (69).] The SU(N) ($\nu_c=0.5$, $\lambda=3$) and U(1) form factors at the quark level are actually rather similar. The difference in normalization is not readily apparent, as for this ν_c and λ the contribution of $F_1(q)$ at $q=0$ is rather small. However, the form factors of the respective hadronic models are distinct from each other level by level in truncation and differ in how they converge to their respective quark models. Figure 5 shows the total form

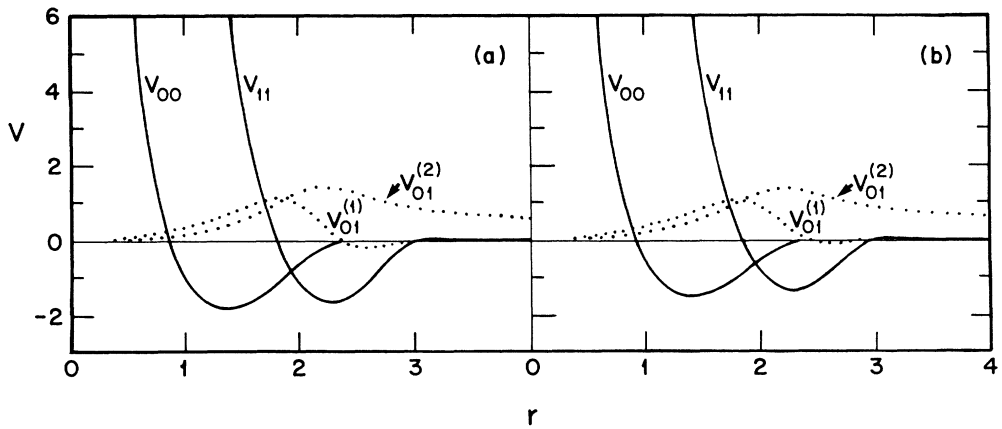

FIG. 4. Effective hadron potentials for the SU(N) (r,θ) schemes [Eqs. (36), (69), and (68)] through $n=m=1$. (a) $\nu_c=0.5$, $\lambda=3$. (b) $\nu_c=0.6$, $\lambda=2$. See Figs. 1 and 2 for conventions.

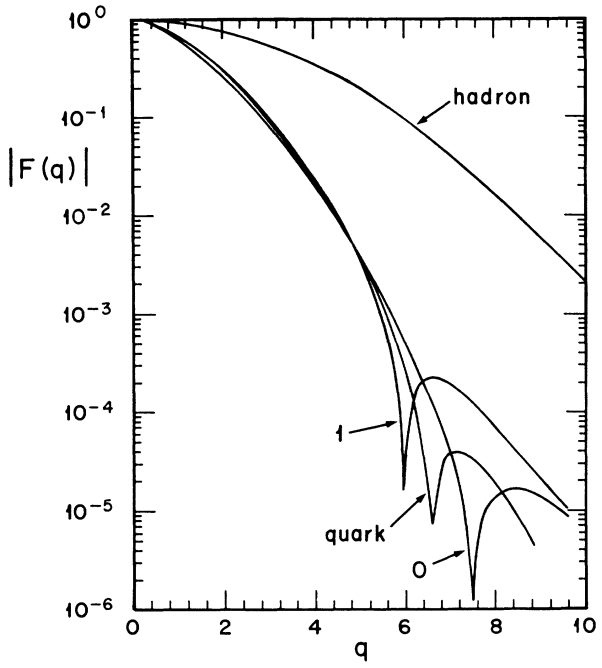

FIG. 5. Effective form factor vs q for truncations $\sigma=0$ and $\sigma=1$ in the SU(N) (r,θ) scheme with $\nu_c=0.5$, $\lambda=3$. "Quark" is the quark-model form factor $F_0(q)$, defined in Eq. (14). "Hadron" is the isolated hadron form factor $|f_{00}(q)|^2=e^{-q^2/16}$ which sets the scale in q. ν_c and λ are defined in the text and in Fig. 2.

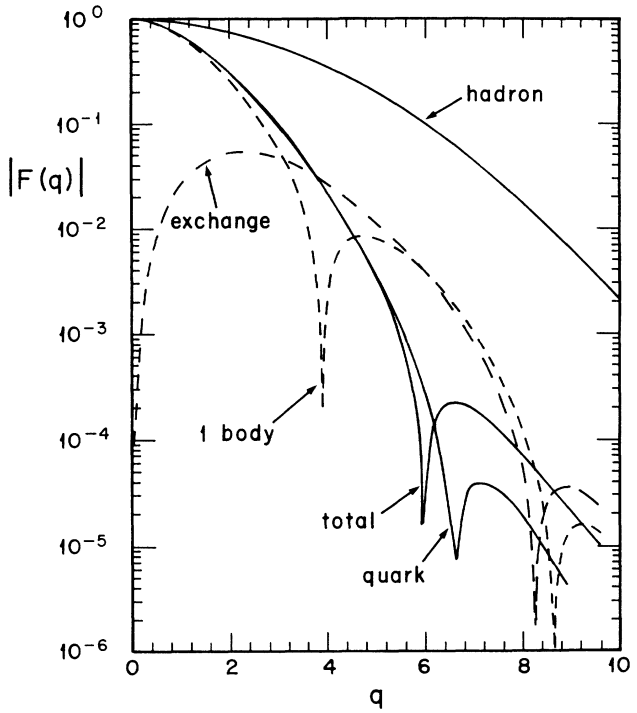

FIG. 6. One-body and exchange contributions to the $\sigma=1$ effective form factor in the SU(N) (r,θ) scheme with $\nu_c=0.5$, $\lambda=3$ vs q. "Quark" and "hadron" are defined in Fig. 5, whereas ν_c and λ are defined in the text and in Fig. 2.

factor for the $\sigma=0$ and $\sigma=1$ truncations for the $\nu_c=0.5$, $\lambda=3$ system against the quark-model form factor. The inclusion of the second channel certainly improves the description of the secondary maximum, although the position of the zero relative to the quark value is only slightly better. This is in contrast to the U(1) results, where the $\sigma=1$ truncation was markedly better than the $\sigma=0$ calculation, and the $\sigma=1$ truncation was in surprisingly good agreement with the quark-model form factor. However, the convergence of the $\sigma=1$ calculation to the quark model in this case is still fairly good, and the agreement found does not change significantly as q increases—even to the point where the isolated hadron form factor has fallen by 2 orders of magnitude. As in the U(1) case, the cancellation of the one-body and exchange contributions gives rise to the convergence seen; this is shown in Fig. 6. All in all the SU(N) (r,θ) hadronization scheme considered converges rather well to the quark-model observables. It is of interest to see how this convergence changes in going to a (y,z) scheme which incorporates $\tilde{g}(t)$ information in merely the ∂_z derivative.

A (y,z) hadronization scheme shall now be considered in which the confined wave functions $\varphi_n(z;y)$ will satisfy the same equations of motion, Eq. (27), and orthonormality conditions as in the U(1) case but now obey the $z=y$ boundary condition

$$\left.\frac{\partial_z\varphi_n(z;y)}{\varphi_n(z;y)}\right|_{z=y=t}=\tilde{g}(t)\ . \tag{79}$$

The $\varphi_n(z;y)$ are calculated via a sine basis expansion. That is,

$$\varphi_n(z;y)=\sum_{m=1}A_m^{(n)}(y)\sin\left[\frac{b_m\pi z}{2y}\right],$$

where the boundary condition Eq. (79) must be satisfied term by term. This yields a transcendental equation for the b_m

$$\frac{b_m\pi}{2}\cot\left[\frac{b_m\pi}{2}\right]=y\tilde{g}(y)\ . \tag{80}$$

The computation of the b_m proceeds as described above. Now, however, there is some trouble for the $\nu_c=0.5$, $\lambda=3$ case. That is, the functional form of the right-hand side of Eq. (80) is such that it does exceed 1 at $y\approx2.44$. At this point, the nodeless solution is lost, and the sine basis expansion becomes hopelessly diseased. Unfortunately, this failure occurs at a sufficiently small y that it is impossible to patch the numerical calculation onto large-y asymptotic forms. Thus, in the work below, I am limited to the $\nu_c=0.6$, $\lambda=3$ and $\nu_c=0.6$, $\lambda=2$ cases. The projector has the same form as in the previous section, Eq. (30), and, concommitantly, the effective Hamiltonian is identical in form to that of the U(1) (y,z) case [see Eq. (35).] Unlike the (r,θ) case, the large-y potential forms depend sensitively on the boundary conditions the $\varphi_n(z;y)$'s satisfy. For small y, the potentials are of identical form to the U(1) case. [See Eq. (39).] $\tilde{g}(y)$ is finite as $y\to0$, so that the right-hand side of Eq. (80) guarantees that the b_m go to the U(1) values of $2m+1$ as $y\to0$.

Now the exchange operator which pertains to the sing-

let form factor is identical in form to Eq. (46). The hidden color effective charge operator can be derived as well. The hadronic expansion of Ψ_0 and $\partial_n\Psi_0$, Eqs. (32) and (79), for $y=z=t$ yields

$$\Psi_0(y,z)\Big|_{y=z=t}=\frac{1}{\sqrt{2}}\sum_n \varphi_n(t;t)\chi_n(t)\ , \tag{81a}$$

$$\partial_n\Psi_0(y,z)\Big|_{y=z=t} =\frac{1}{\sqrt{2}}\sum_n \{[\bar{g}(t)\varphi_n(t;t)-\partial_y\varphi_n(t;y)|_{y=t}]\chi_n(t) -\varphi_n(t;t)\partial_t\chi_n(t)\}\ . \tag{81b}$$

The normal derivative from $y>z$ has been considered. Introducing

$$C_n(t)\equiv\bar{g}(t)\varphi_n(t;t)-\partial_y\varphi_n(t;y)|_{y=t}\ , \tag{82}$$

it is clear from the form of the normal derivative on $y=z=t$, that $C_n(t)-\varphi_n(t;t)\cdot\vec{\partial}_t$ plays the role that

$$\frac{r}{\sqrt{2}}\bar{g}\left[\frac{r}{\sqrt{2}}\right]\varphi_n(\pi/4;r)$$

played in the (r,θ) case. Using Eq. (75), one obtains

$$\rho^{\rm hc}_{nm}(t',t'')=\frac{e^{-q^2/32}}{\beta^2}\{[C_n(t')-\vec{\partial}_{t'}\cdot\varphi_n(t';t')]\tilde{\alpha}(t',t'')(\alpha+s)^2[C_m(t'')-\varphi_m(t'';t'')\cdot\vec{\partial}_{t''}] -(\alpha^2-1)\varphi_n(t';t')\tilde{\beta}(t',t'')[C_m(t'')-\varphi_m(t'',t'')\cdot\vec{\partial}_{t''}] -[C_n(t')-\vec{\partial}_{t'}\cdot\varphi_n(t';t')](\alpha^2-1)\tilde{\beta}(t'',t')\varphi_m(t'';t'')+(\alpha-s)^2\tilde{\gamma}(t',t'')\varphi_n(t';t')\varphi_m(t'';t'')\}\ . \tag{83}$$

$\rho^{\rm hc}_{nm}(t',t'')$ is more complicated than in the (r,θ) case simply because the confined coordinate z for $y>z$ is not the normal coordinate at the rearrangement surface $z=y$. The $\tilde{\alpha}$, $\tilde{\beta}$, and $\tilde{\gamma}$ are now

$$\int_0^\infty dy\int_0^y dz\, j_0\left[\frac{q}{2}y\right]j_0\left[\frac{q}{2}z\right]G_1(y,z,t',t')G_I(y,z,t'',t'')\equiv\tilde{\alpha}(t',t'') \tag{84a}$$

$$\int_0^\infty dy\int_0^y dz\, j_0\left[\frac{q}{2}y\right]j_0\left[\frac{q}{2}z\right]G_I(y,z,t'',t'')\Gamma_I(y,z,t',t')\equiv\tilde{\beta}(t',t'')\ , \tag{84b}$$

$$\int_0^\infty dy\int_0^y dz\, j_0\left[\frac{q}{2}y\right]j_0\left[\frac{q}{2}z\right]\Gamma_I(y,z,t',t')\Gamma_I(y,z,t'',t'')\equiv\tilde{\gamma}(t',t'')\ . \tag{84c}$$

$\rho^{\rm hc}_{nm}(t',t'')$ is finite at $q=0$; its physical interpretation is as described above. I have not calculated the hidden color exchange charge; again, as in the (r,θ) case, consideration is restricted to the color singlet portion of the form factor $F_0(q)$.

The potentials for the $\nu_c=0.6$, $\lambda=3$ case through $n=m=1$ are shown in Fig. 7. The channel potentials are strikingly less attractive than in the commensurate U(1) case. This is supported by a large-y calculation of $\varepsilon_0(y)-\varepsilon_0(\infty)$, using the techniques outlined in Sec. III A. That is,

$$\varepsilon_0(y)-\varepsilon_0(\infty)\sim-32\sqrt{2/\pi}y^3e^{-2y^2}\times\left[1+\bar{g}(t)\frac{1}{y}+O(y^{-2})\right]\ . \tag{85}$$

The term in brackets multiplies the U(1) form of $\varepsilon_0(y)-\varepsilon_0(\infty)$ [see Eq. (58)]. An explicit evaluation of this multiplicative factor at $y=3$ yields 0.70 for the $\nu_c=0.6$, $\lambda=3$ case, so that in asymptotia the SU(N) potentials are

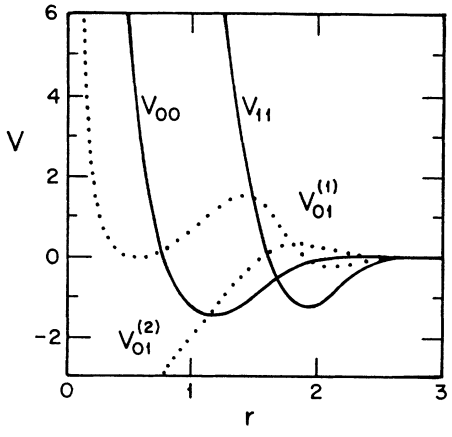

FIG. 7. Effective hadron potentials through $n=m=1$ for the SU(N) (y,z) scheme [Eqs. (35), (79), and (68)] with $\nu_c=0.6$, $\lambda=3$. See Figs. 1 and 2 for conventions.

less attractive than the U(1) ones. This decreased attraction is reflected in the calculation of the binding energy. At the $\sigma=2$ truncation, the system has *no* bound state; nor is the $\nu_c=0.6$, $\lambda=2$ case bound at this level. The boundary values the SU(N) confined wave functions incorporate are nontrivial, so that it seems that the hadronizations in this case are much more sensitive to the incorporation of the correct boundary conditions at $z=y$. These results seem to indicate that the incorporation of the correct boundary conditions in the confined wave functions is essential in establishing convergence to the SU(N) quark-model results.

V. CONCLUSIONS

The above results show that a parameter-free hadronic description with a small number of hadronic degrees of freedom can reproduce the quark-model observables with remarkable accuracy—for both U(1) *and* SU(N) color dynamics. The SU(N) results reproduce the general features seen at the U(1) level. That is, the (r,θ) scheme which incorporates the exact SU(N) boundary condition converges well to both the quark-level binding energy and form factor for the choice of $\nu_c=0.5$, $\lambda=3$ color dynamics. The convergence is likely not accidental; the calculation of the scattering lengths at the $\sigma=0$ level for the $\nu_c=0.5$, $\lambda=3$; $\nu_c=0.6$, $\lambda=3$; and $\nu_c=0.6$, $\lambda=2$ cases show the agreement to the respective quark-level calculations to be roughly equivalent. This is important as comparison of the hadron-scheme and quark-model results for different sets of ν_c and λ are necessary in order to gauge the sensitivity of the convergence to the particular number of colors—here $N=2$ or 3—or, by dialing the strength parameter ν_c, to the form chosen for the color nonsinglet interactions. The form-factor convergence seen for the $\nu_c=0.5$, $\lambda=3$ case is perhaps not as dramatic as in the U(1) limit, but it persists to the same high q. At $q=8$, the isolated hadron form factor is already $O(10^{-2})$, but the form factor of the $\sigma=1$ truncation of the hadronic basis is $O(10^{-4})$ and yet continues to reproduce the form factor's qualitative structure. The potentials in this hadronic scheme are identical to those of the U(1) case as $r\to 0$ or as $r\to\infty$. The potentials vary from those of the U(1) case only for intermediate r, and, essentially, only the overall size of the $n=m$ potential minima are modified. The repulsion for small r, as in the U(1) case, comes from the imposition of a boundary condition at $\theta=\pi/4$, from inclusion of the exchange dynamics. A significant departure from the qualitative features seen in the U(1) case is the poor convergence of the (y,z) scheme with the

$$\partial_z\varphi_n(z;y)|_{z=y=t}=\tilde{g}(t)\varphi_n(t;t)$$

constraint at the rearrangement surface. The U(1) version of this scheme does as well as the corresponding (r,θ) scheme; here, however, the $n=m=2$ truncation of the hadronic basis for the $\nu_c=0.6$, $\lambda=3$ case is not even bound. At the SU(N) level, the incorporation of the exchange dynamics is necessary, but no longer sufficient; the incorporation of the exact boundary condition in the confined coordinate is now essential—at least in the limited set of examples explored.

At neither the U(1) nor SU(N) levels does this study provide encouragement for any distinctive quark signatures in low-energy nuclear observables. The rapid convergence of the (r,θ) hadronic description to the high-q SU(N) form factor has been discussed above. In the U(1) limit, the efficacy of the hadronic expansion persists for both the second moment of the momentum distribution and the high-q form factor; this is contrary to all naive expectations as $n(p)$ and $F(q)$ are rather different probes of the bound state's structure. The convergence is rapid not only for $F(q)$; $\langle p^2\rangle$ is reproduced very well in $\sigma=1$ for the two schemes considered, even though $n(p)$ of an inert meson description in lowest order has incorrect low-p behavior. That these parameter-free descriptions are successful in describing the $q^2\bar{q}^2$'s bound state is not the only surprise; at the U(1) level, a rather remarkable feature is the scheme independence of the convergence. The (y,z) and (r,θ) schemes both incorporate the quark-exchange dynamics but differ qualitatively in the large-r behavior of their potentials and two-body charge operators; however, they converge nearly as well to the quark-level results. This insensitivity to the particular hadronic scheme demonstrates that the convergence found is likely not accidental and strengthens a general conclusion as to the presence of quark signatures in low-energy nuclear observables. This feature could not be demonstrated in the SU(N) case because of the sensitivity of the results there to the precise boundary condition imposed on the confined coordinate. The comparison of the scattering lengths of the SU(N) (r,θ) schemes in $\sigma=0$ for various ν_c and λ with their respective quark-level values shows at least no strong sensitivity to the particular ν_c and λ chosen.

There may be no distinctive quark signatures in low-energy nuclear observables, but this is not a negative result. Quite the contrary, it gives credibility to programs which would attempt to calculate "observed" hadronic phenomenological parameters from the underlying theory. In addition, it is to be emphasized that, regardless of the sophistication of such attempts, a consistent, understood, hadronization scheme is a necessary underpinning of any such calculation. I point to the important role of the exchange charge in yielding the convergence to the high-q form factor in making this statement. The channel wave functions alone in any scheme, represented here by the convolution model form factor, are not by any means sufficient to describe this process. The general requirements of a consistent hadronization scheme should apply as well to a lattice calculation as to a potential quark model.

Other low-energy nuclear observables exist which probe slightly different aspects of the $q^2\bar{q}^2$'s bound state. One interesting probe is the response function $R(\omega,q)$ at mismatched kinematics, say for small, but finite, ω and large q. Kumano has compared the response of a $q^2\bar{q}^2$ system with quark-exchange dynamics in an overall harmonic confining potential to that of a hadronic version of the same model, and has found the hadronic description to persist to large values of q.[12] That model study was

performed solely in the context of U(1) color dynamics; this is a chance for the inclusion of the hidden color sector to wreak havoc with the good agreement found at the U(1) level. The similarity of U(1) and SU(N) results for the hadronic form-factor convergence has little bearing on this situation; the response function for these mismatched kinematics is a distinct observable.

One interesting dimension that could be explored is the study of a SU(N) quark-exchange model with dynamics that carry over to a system of noninteracting mesons for sufficiently large N. The prescription of Ref. 2 for the hidden color forces which is used here does not have this nice property. Masutani has studied the quark-exchange model for $q^2\bar{q}^2$ using hidden color interactions that have the appropriate large-N behavior.[8] He chose a Hamiltonian of form

$$h(y,z)=-\partial_y^2-\partial_z^2+4[z^2P_0+y^2\tilde{P}_0+\nu_c^2(y^2P_1+z^2\tilde{P}_1)] \tag{86}$$

with $\nu_c=1$. This Hamiltonian contains only noninteracting mesons in large N since $|1\rangle\equiv|\tilde{0}\rangle$ for an infinite number of colors. As is consistent with the ideas of 't Hooft and Witten, he found the meson-meson scattering amplitude to go as $1/N$ for large N. This suggests the following interesting program: one could "hadronize" his model and explore the hadronic expansion convergence for low-energy observables as a function of N to test in a model context the idea that the large-N, low-E phenomenology of the Skyrme model is applicable at $N=3$. The trouble is that the Masutani model admits no bound states for $\nu_c=1$. Perhaps the model would have bound states for $\nu_c<1$ as in the Lenz *et al.* model, but its nice large-N properties would then vanish. However, a study of the low-energy scattering observables might be interesting.

ACKNOWLEDGMENTS

I am indebted to E. J. Moniz for his advice and guidance throughout the course of this project. I also thank S. E. Koonin for his hospitality at Caltech, where some of this work was completed. This work was primarily supported by the U.S. Department of Energy (DOE) under Contract No. DE-AC02-76ER03069, with partial support from the Bundesministerium für Forschung and Technologie (BMFT) under Contract No. 06-HD-710.

---

*Present address: Institut für Theoretische Physik der Universität Heidelberg, Philosophenweg 19, D-6900 Heidelberg, Federal Republic of Germany.

[1]S. Gardner and E. J. Moniz, Phys. Rev. C **36**, 2504 (1987).

[2]F. Lenz, J. T. Londergan, E. J. Moniz, R. Rosenfelder, M. Stingl, and K. Yazaki, Ann. Phys. **170**, 65 (1986).

[3]G. 't Hooft, Nucl. Phys. **B72**, 461 (1974); **B75**, 461 (1974).

[4]E. Witten, Nucl. Phys. **B160**, 57 (1979).

[5]N. Isgur, in *Soft QCD: Low Energy Hadron Physics with Chromodynamics,* Proceedings of the 16th International School of Subnuclear Physics, Erice, 1978, edited by A. Zichici (Plenum, New York, 1980), p. 107.

[6]O. W. Greenberg and H. J. Lipkin, Nucl. Phys. **A370**, 349 (1981).

[7]G. Feinberg and J. Sucher, Phys. Rev. D **20**, 1717 (1979).

[8]K. Masutani, Nucl. Phys. **A468**, 593 (1987).

[9]A. Erdelyi *et al.*, *High Transcendental Functions* (McGraw-Hill, New York, 1953), Vol. 1.

[10]I. M. Gradshteyn and I. M. Ryzhik, *Tables of Integrals, Series, and Products* (Academic, New York, 1980), p. 495.

[11]R. Rosenfelder (private communication). The odd behavior of these functions for $r\gtrsim 3$ is undoubtedly due to the mere five significant figure precision of the $\phi_n^{l=1}(t)$ expansion coefficients. A set of ten functions was used for the calculation; the cancellation is sensitive to the accuracy of the coefficients at large t. If the effective potentials found are of sufficiently short range, the behavior of these functions will likely only be needed to $t=3$.

[12]S. Kumano, Ph.D. thesis, M.I.T., 1985 (unpublished).